HHS Public Access

Author manuscript

Biochem Soc Trans. Author manuscript; available in PMC 2024 June 28.

Published in final edited form as:

Biochem Soc Trans. 2023 June 28; 51(3): 897–923. doi:10.1042/BST20210699.

Structures and coordination chemistry of transporters involved in manganese and iron homeostasis

Shamayeeta Ray,

Rachelle Gaudet

Department of Molecular and Cellular Biology, Harvard University, Cambridge, MA 02138 USA

Abstract

A repertoire of transporters plays a crucial role in maintaining homeostasis of biologically essential transition metals, manganese and iron, thus ensuring cell viability. Elucidating the structure and function of many of these transporters has provided substantial understanding into how these proteins help maintain the optimal cellular concentrations of these metals. In particular, recent high-resolution structures of several transporters bound to different metals enable an examination of how the coordination chemistry of metal ion-protein complexes can help us understand metal selectivity and specificity. In this review, we first provide a comprehensive list of both specific and broad-based transporters that contribute to cellular homeostasis of manganese (Mn^{2+}) and iron (Fe^{2+} and Fe^{3+}) in bacteria, plants, fungi, and animals. Further, we explore the metal-binding sites of the available high-resolution metal-bound transporter structures (Nramps, ABC transporters, P-type ATPase) and provide a detailed analysis of their coordination spheres (ligands, bond lengths, bond angles, and overall geometry and coordination number). Combining this information with the measured binding affinity of the transporters towards different metals sheds light into molecular basis of substrate selectivity and transport. Moreover, comparison of the transporters with some metal scavenging and storage proteins, which bind metal with high affinity, reveal how the coordination geometry and affinity trends reflect the biological role of individual proteins involved in homeostasis of these essential transition metals.

Introduction

All living cells require transition metals in low intracellular concentrations for various biological processes. Cellular metal levels are tightly regulated as imbalances in their optimal concentrations cause several diseases [1,2]. In this review, we focus on two abundant and essential transition metals, manganese and iron, neighbors on the periodic table and thus closely related. Manganese is a cofactor of vital enzymes including superoxide dismutase (SOD) which breaks down reactive oxygen species (ROS) and glutamate synthetase involved in mammalian brain development and function [3,4]. Manganese is also important in processes like bone and tissue growth, reproduction, and immune system function [5,6]. Manganese overload in the brain leads to a condition called ‘manganism’ with Parkinson-like symptoms [6-8]. In plants, manganese catalyzes photooxidation of

Correspondence: Rachelle Gaudet (gaudet@mcb.harvard.edu).

water by photosystem II during light reactions and provides structural integrity to various photosynthetic proteins and enzymes [9-11]. Manganese is also crucial for bacterial survival and growth, and virulence of pathogenic bacteria [12,13]. During pathogenesis, manganese (with or without SOD) protects the microbes from host-mediated oxidative stress by detoxification of ROS [4,14].

Iron, in ionic form or as part of a complex, is an essential cofactor of proteins involved in many processes including oxygen transport and storage, electron transport and catalysis, cellular and oxygen metabolism, DNA synthesis and repair, cellular signaling, and host defense [15-17]. Iron deficiency causes restricted erythropoiesis and anemia [17-20]. Elevated iron is also problematic, for example in organs it causes tissue damage (hemochromatosis), in the blood it leads to atherosclerosis, and in the brain causes neurodegeneration [17,21,22]. In cyanobacteria, algae, and plants, iron is the predominant metal in the photosynthetic machinery, and it contributes to electron transport and chlorophyll biosynthesis [23-25]. In stress conditions, iron imbalances generate ROS and impair plant growth, photosynthesis, electron transport [10,25,26].

Organisms have evolved tightly regulated systems to maintain optimal metal concentrations in cellular compartments. The metal homeostasis machinery includes: (i) transporters and ion channels that import and export metals across otherwise impermeable cellular and organellar membranes, (ii) metallochaperones and chelators that store and retain metals in certain compartments, and (iii) transcription factors, sensors, and riboswitches that regulate the expression of genes encoding for the homeostasis machinery [27,28]. Metal homeostasis necessitates that this machinery can select appropriate metals over others [27-29]. The coordination chemistry, geometric preferences, and chemical properties—like atomic and ionic radii, electronegativity—of individual metals are key contributors to this specificity [2,27,30]. However, according to the Irving-Williams series ($Zn^{2+} < Cu^{2+} > Ni^{2+} > Co^{2+} > Fe^{2+} > Mn^{2+}$), a transition metal ion higher in the series tends to form more kinetically or thermodynamically stable protein-metal complexes and can potentially displace metals that are downstream in the series [31,32]. Hence, transition metal transporters often have a broad substrate scope even when physiologically implicated in homeostasis of a particular metal [27,28,33,34].

In this review, we address the factors driving selective iron and manganese transport and homeostasis. We first explore the transporters and receptors that contribute to manganese and iron homeostasis in mammals, yeasts, plants, and bacteria. From the list, we analyze the structures of different manganese- and iron-bound proteins available at high resolution to understand how structures correlate to biological function and factors that drive metal ion selectivity. Detailed analysis of the metal coordination spheres and their deviation from ideal parameters for different bound metals illustrates how the protein discriminates its cognate substrates from non-physiological ones. Reviewing the published affinities of metals to different proteins (either K_m or K_d), we find that they mostly, but not always, correlate to the ideality of the coordination geometries. Overall, we show that the combined knowledge of coordination structures and binding affinity can help understand the function of the key players involved in manganese and iron homeostasis.

Overview of manganese transporters in different organisms

Before we discuss the structural analyses, we briefly introduce the families of receptors and transporters—*importers* that bring substrates into the cytosol and *exporters* that ferry substrates from the cytosol to lumenal compartments or the extracellular space—implicated in manganese homeostasis. These players in manganese homeostasis are illustrated in Figure 1, listed in Table 1, and described by organism type below.

Bacteria

Most importers and exporters contributing to manganese homeostasis are ubiquitously present in both gram-positive and gram-negative bacteria (Figure 1A, Table 1). Mn^{2+} importers include ATP-binding cassette (ABC) transporters, such as SitABC and PsaABC, that use energy derived from ATP hydrolysis, and a Natural resistance associated macrophage protein (Nramp) homolog, MntH, that uses co-transported protons as an energy source [12,33,34]. In *Bradyrhizobium japonicum*, a porin, MnoP, is coregulated with MntH and assists in Mn^{2+} diffusion across the outer membrane (OM) during Mn^{2+} deprivation [27,35]. Mn^{2+} exporters include: cation diffusion facilitator (CDF) family H^{+} antiporters like MntE, MntP, and YiiP [36,37]; P_{II} -type ATPases like YoaB and MgtA [12,13,27]; TerC-type proteins like YkoY [12,13,38]; MntP-type proteins; and the major facilitator superfamily (MFS) transporter FPN, a homolog of human ferroportin [39-41]. To maintain homeostasis, the expression levels of transporter genes are regulated by either or both riboswitches like yybP-ykoY [12,42] and transcription factors like MntR [12,43].

Plants

In plants, many transporters contribute to Mn^{2+} uptake through the roots and distribution in cells of various tissues and intracellular organelles (Figure 1B, Table 1) [9,11]. Mn^{2+} importers include Nramps like *Oryza sativa* (Os)Nramp3/5, *Arabidopsis thaliana* (At)Nramp1 (plasma membrane; PM) and AtNramp3/4 (vacuole) [9-11]. Yellow stripe-like (YSL) importers, belonging to oligopeptide transporter (OPT) family, mediate long-distance uptake of Mn^{2+} in complex with nicotianamine (e.g., AtYSL4/6, OsYSL2/6) [9,44]. Zrt-/Irt-like proteins (ZIPs) have a broad substrate scope including Zn^{2+}, Fe^{2+}, and Mn^{2+}, with IRT1 (PM), ZIP1 (vacuole), and ZIP2 (PM) most strongly associated with Mn^{2+} import in *A. thaliana* [9,11,45]. The exporters that internalize Mn^{2+} in intracellular compartments include: cation exchangers (CAX) expressed in vacuoles in plants exposed to toxic Mn^{2+} levels (e.g., AtCAX2/4/5) [9,46]; CDFs (also known as MTP in plants; e.g., AtMTP11, OsMTP8.1) [9,47]; P-type Ca^{2+}-ATPases like AtECA1 (endoplasmic reticulum; ER) and AtECA3 (Golgi) [9-11]; and vacuolar iron transporter (VIT) subfamily of Ca^{2+}-sensitive cross complementer1 (CCC1) transporters in vacuoles and the Golgi (e.g., ATVIT1, OsVIT1/2) [48-50].

Fungi

The fungal Mn^{2+} homeostasis machinery has been most extensively studied in yeasts (Figure 1C, Table 1) [2,51]. Mn^{2+} importers include: Nramps like Smf1 (PM) and Smf2 (intracellular vesicles and ER) [52-54]; Mnc1, a CYSTM (non-secreted cysteine-rich peptide) family member that chelates manganese at the cell surface [55]; Pho84, a

phosphate/proton MFS symporter which transports Mn^{2+} as $MnHPO_4$ in high environmental Mn^{2+} conditions [56]; and a ZIP transporter, Atx2, traffics Mn^{2+} out of Golgi vesicles [51,57,58]. To limit cytosolic Mn^{2+}, several exporters internalize Mn^{2+} into intracellular compartments: P-type ATPases Pmr1 (Golgi), Ypk9 (vacuole) and Cod1 (ER) [52,54,59]; CCC1 exporters Ccc1 (vacuole) [52-54]; CAX exporter Gdt1 (Golgi) [60,61] and the mitochondrial carrier (MC)-family exporter Mtm1 (mitochondria) [62].

Animals

Animals use manganese (Mn^{2+} or Mn^{3+}) homeostasis machinery for several essential life processes and for nutritional immunity against invading pathogens (Figure 1D, Table 1) [7,28,39]. The immunity proteins include the Nramp-family namesake, NRAMP1, which extrudes Mn^{2+} and Fe^{2+} out of the phagosomes of macrophages into the cytosol to deplete the engulfed pathogens of essential nutrients [34,39,63]. Mn^{3+} is carried in the bloodstream by transferrin (whose preferred substrate is Fe^{3+}) then internalized into endosomes by the transferrin receptor (TfR), where Mn^{3+} is released and converted to Mn^{2+} by STEAP metalloreductases [34,64,65]. The main Mn^{2+} importers are NRAMP2, involved in uptake from endosomes and the PM [66], and ZIP8 and ZIP14, importing Mn^{2+} preferentially over Zn^{2+} and Fe^{2+} across the PM [28,67]. The main Mn^{2+} exporters are: P-type ATPases ATP13A2 (Park9; lysosomes) [28,68] and SPCA1 (Golgi) [28,69]; CDF-family transporter ZNT10 (Zinc transporter 10) that preferentially exports Mn^{2+} over Zn^{2+} across the PM [28,53,67]; CAX-family TMEM165 (Golgi) [28,60,70]; and the MFS transporter, ferroportin [28,71] and the MC-family MFRN1 and MFRN2 that import Mn^{2+} into the mitochondria in Fe^{2+} deficiency conditions [28,72].

Manganese is vital to brain function and its dyshomeostasis induces neurological disorders [6,28,39]. Accordingly, the generic cell in Figure 1D also includes many channels and transporters that primarily shuttle other substrates but have been implicated in Mn^{2+} fluxes in brain tissues (reviewed in [6,73]). These include store-operated Ca^{2+} channels (SOCs), voltage-gated calcium channels, ionotropic glutamate receptors (NMDARs), the electrogenic amino acid transporter (EAAT) family of glutamate and glutamine transporters, the dopamine transporter (DAT), MFS-family monocarboxylate transporter (MCT), and Huntingtin-interacting proteins HIP14 and HIP14L (Mg^{2+} transporters expressed in the Golgi).

Structural insights into manganese transport

Transporters involved in Mn^{2+} homeostasis either use Mn^{2+} as their primary substrate but can also transport other transition metals (e.g., MntH, PsaABC, SitABC) [74-76], or moonlight as Mn^{2+} transporters, as do most Fe^{2+} transporters (e.g., TfR, ferroportin), sometimes under dyshomeostasis conditions [41,64,77], and some Zn^{2+} transporters (ZNT10, ZIP8/14) [67]. In both cases, it will be useful to understand what drives Mn^{2+} selection in a physiological context. Mn^{2+} prefers an octahedral geometry, with optimal bond lengths of 2.1-2.5 Å as ‘strong interactions’, although longer bond lengths of 2.5-3.0 Å can still participate in a coordination sphere as ‘weak interactions’ [78-80]. However, chelation of Mn^{2+} can be constrained by the protein structure to differ from ideal

coordination geometry; it is therefore important to visualize Mn^{2+}-interactions to understand how it influences function. Although several Mn^{2+} transporter structures are available, few are high-resolution metal-bound structures (Table 1 and 2). Recent high-resolution structures of ABC transporter SBPs, P-type ATPases and Nramps are beginning to shed light on the key factors that drive Mn^{2+} specificity [31,75,81]. We summarize this progress below, as well as sequence analyses that provide clues regarding Mn^{2+} specificity for transporters like ZNT10 and ZIP8/14 [67].

MntR

We first set the stage by examining the structure of MntR, the bacterial transcription regulator of genes important for Mn^{2+} biology and homeostasis [43,82]. In contrast to transporters that interact with metal ions only transiently, MntR is effectively a switch regulated by high-affinity Mn^{2+} binding. MntR coordinates Mn^{2+} in a near-ideal octahedral geometry favored by Mn^{2+} (Figure 2A-C, Table 2) [83,84]. The metal-oxygen and metal-nitrogen coordinating bond lengths are within the ‘strong interaction’ range [78,85]. This near-ideal coordination of Mn^{2+} by MntR reflects its high affinity for Mn^{2+} (K_d of 0.2–2 μM) [83], and its function as a Mn^{2+}-regulated switch.

SBPs

Structures of bacterial ABC transporter SBPs that import Mn^{2+}—*Streptococcus pneumoniae* PsaA *Staphylococcus pseudintermedius* SitA—bound to different metals shed light on their metal-binding properties (Figure 2D) [31,75]. Both Mn^{2+} and Zn^{2+} bind at the same site in PsaA. The coordination geometry has been assigned as tetrahedral in both cases [31], although two additional oxygens at 2.4 Å—still within the ‘strong interaction’ range [78-80]—can be included to the Mn^{2+} sphere to produce an alternative distorted octahedral coordination (Figure 2E-F, Table 2). Mn^{2+} prefers octahedral and Zn^{2+}, tetrahedral geometry [27,30]. Thus, Mn^{2+} binds PsaA in a non-ideal coordination geometry and with greater angular deviations than Zn^{2+} (Table 2). Based on the metal-free structure of the transporter domain, PsaC, its proposed metal-binding site includes two aspartates and two histidines, potentially forming a coordination sphere similar to its SBP, PsaA [86]. Interestingly, PsaABC transports Mn^{2+} and not Zn^{2+} although both metals bind PsaA with high affinity (K_d = 3.3 ± 1.0 nM for Mn^{2+} and K_d = 231 ± 1.9 nM for Zn^{2+}; Table 2) [87]. These data suggest that the binding-site distortions may enable the conformational switching between different states of PsaA essential for Mn^{2+} transport. In contrast, the ideal geometry and higher thermal stability of the Zn^{2+}-bound PsaA complex indicate reduced conformational flexibility [31]. Thus, Zn^{2+} appears to lock PsaA in a closed state and prevents transport [31]. In sum, the coordination geometries of the PsaA-metal complexes are key for selective transport of Mn^{2+} over Zn^{2+} by PsaABC, but also make *Staphylococcus pneumoniae* susceptible to Zn^{2+}, which can inhibit the acquisition of the essential metal Mn^{2+} [31,88].

In the SitA case, Mn^{2+} and Zn^{2+} are both octahedrally coordinated with the same ligands, a coordination geometry preferred by Mn^{2+} but not Zn^{2+} (Figure 2G-H, Table 2) [75]. Moreover, some bonds to Zn^{2+} are longer than the optimal 2.0–2.2 Å and the coordination sphere is more distorted for Zn^{2+} than Mn^{2+} (Table 2). Although SitA binds both metals in the nM range (Table 2), the coordination geometries indicate that its binding site is better

adapted to accommodate Mn^{2+}. The MntC SBP also binds its preferred substrate, Mn^{2+}, in an ideal octahedral coordination [89].

These SBP structures demonstrate that selective Mn^{2+} transport by bacterial ABC transporters is likely related to how Mn^{2+} and potential competing substrates are coordinated by the SBP. However, formation of an ideal coordination sphere does not necessarily result in effective transport. For example, effective transport of Mn^{2+} likely also depends on how readily the Mn^{2+} can be released from the SBP by the transmembrane subunits of the transporter, at least in the case of PsaA.

P-type ATPase

Human SPCA1, a P-type ATPase that exports both Ca^{2+} and Mn^{2+} from cytosol into the Golgi, with similar K_m values of 70 nM for Mn^{2+} and 130 nM for Ca^{2+} [90]. Cryo-EM structures of SPCA1 reveal how Ca^{2+} and Mn^{2+} bind with different geometry to the same site in the transmembrane domain (Figure 2I-K) [91]. Both metals bind with all oxygen ligands, with a 6-ligand octahedral geometry for Ca^{2+} and 5-ligand square pyramidal geometry for Mn^{2+} (Table 2), although in both cases, a potential water molecule ligand can be accommodated, which would generate a 7-ligand pentagonal bipyramid geometry commonly observed in Ca^{2+} coordination, and 6-ligand octahedral coordination for Mn^{2+}. Bond lengths are smaller for Mn^{2+} than Ca^{2+} consistent with its smaller ionic radius. The small angular deviations and near-ideal bond length are consistent with the low K_m values for both substrates.

Nramps

In the bacterial *Deinococcus radiodurans* (Dra)Nramp, the physiological substrate Mn^{2+} and the non-essential substrate Cd^{2+} bind the same site, both in an octahedral geometry (Figure 2L-N) [81], although octahedral and tetrahedral geometries are the preferred coordination for Mn^{2+} and Cd^{2+} respectively [27,30]. Moreover, the angular deviations are higher for Cd^{2+} (Table 2). The coordinating ligands also differ, with different water arrangements and the aspartate sidechain (D56) in a different rotamer such that it coordinates Mn^{2+} but not Cd^{2+}. This lack of coordination is consistent with Cd^{2+} being a softer metal than Mn^{2+}, with lower propensity to bind harder oxygen ligands. This aspartate is essential for both metal and associated proton transport [34], and its interaction with Mn^{2+} may provide a mechanism to coordinate proton and metal transport. Interestingly, some coordinating bonds for Mn^{2+}, and even more for Cd^{2+}, are longer than ideal (Figure 2M-N). Metal-oxygen distances of 2.1-2.5 Å for Mn^{2+} and 2.3-2.8 Å for Cd^{2+} (0.2 Å longer for metal-sulfur) are considered ‘strong interactions.’ However, longer bonds of 2.6-3.2 Å for Mn^{2+} (and accordingly for Cd^{2+}) are occasionally observed and considered ‘weak interactions’ still important for the overall coordination geometry [78].

DraNramp has relatively low affinity for both metals with K_d values in the ~100 μM range (Table 2; [81]). These are consistent with the observed non-ideal bond lengths and angles. The higher affinity for Cd^{2+} than Mn^{2+} is, at first glance, counterintuitive considering that Mn^{2+} is the physiological substrate and it binds with closer-to-ideal geometry. However, a lower affinity may lead to more favorable metal release kinetics to continue the transporter

cycle. These data also suggest that information on substrate-binding affinity is useful, but often does not provide the full picture and additional factors are at play, like the energetics of the protein conformation.

Another interesting observation from the structures of DraNramp in different conformations is that the physiological substrate, Mn^{2+}, binds at the same site but with different coordination geometries across the various biologically relevant conformations of its transport cycle (Figure 3) [81]. DraNramp is the only transporter for which Mn^{2+}-bound structures are available in multiple conformations. All three (outward-open, occluded, and inward-open) conformations have octahedral Mn^{2+} coordination with substantial angular deviations. Interestingly, the bond lengths are longer and angular deviations are larger in the inward-open which is primed to release Mn^{2+} into the cytosol (Figure 3).

CDF and ZIP transporters

While most CDF-family ZNT exporters selectively transport Zn^{2+}, ZNT10 is implicated in Mn^{2+} transport in mammals [28,67]. A structure of Zn^{2+}-bound human ZNT8 (Figure 4A), a Zn^{2+} transporter, confirms that the conserved HD-HD motif comprising two aspartates and two histidines forms the Zn^{2+}-binding site (Figure 4B) [67,92]. In the absence of experimentally determined ZNT10 structures, sequence analysis suggests that an asparagine replaces one histidine to yield a ND-HD metal-binding motif [67]. This substitution may provide a hard oxygen ligand to bind the harder Mn^{2+} ion, and the asparagine could also form a bidentate interaction to expand its coordination sphere (Figure 4C).

Among the mammalian ZIP family of Zn^{2+} importers, ZIP8 and ZIP14 can transport both Mn^{2+} and Zn^{2+} [67,93]. Structure of a bacterial ZIP transporter reveals the Zn^{2+} transport site (Figure 4D) [93], but in absence of human ZIP structures, sequence analyses provide clues about how ZIP8 and ZIP14 can transport Mn^{2+} [67,93]. Similarly, to the ZNT case above, in ZIP8 and ZIP14 a glutamate replaces the first histidine in the HEXPHEXGD motif conserved in TM5 of LIV-1-subfamily ZIPs (Figure 4E-F) [67]. This glutamate could provide one or two additional oxygen ligands to a Mn^{2+} coordination sphere.

Overview of iron transporters in different organisms

The key players in iron (Fe^{2+}/Fe^{3+}) homeostasis include transporters that transport iron in ionic or in complex form into and out of the cells and its compartments and receptors that bind and transport iron-bound complexes to their appropriate destinations (Figure 4, Table 3). Owing to the similarity in metal ion properties, there is a substantial overlap between iron and manganese transporters [28,64]. Since we have already introduced these overlapping transporters in the section on manganese transporters above, we will focus below on the proteins that are exclusively involved in iron homeostasis.

Bacteria

Iron is transported across the bacterial membrane mostly in complex form and sometimes in ionic Fe^{2+} form (Figure 5A, Table 3). In gram-negative bacteria, Fe^{3+}-siderophores, Fe^{2+}-heme, and Fe^{3+}-transferrin iron is trapped at the OM by β-barrel protein receptors [27,29,94]. The TonB-ExbB-ExbD system energizes iron transport from the OM receptors

across the periplasm to the inner membrane (IM) [27,95,96]. In both gram-negative and gram-positive bacteria, SBPs capture the complexed (siderophore with Fe^{3+} and heme with Fe^{2+}) and ionic (transferrin with Fe^{3+}) iron and their associated ABC transporters import iron into the cytosol [29,95,97]. Ionic Fe^{2+} in gram-negative bacteria is imported by OM porins and then by a GTPase, FeoB, across the IM [95,98,99]. Fe^{2+} export across the IM is mediated by the MFS-family transporter, FPN [41,100,101]; and the CDF-family YiiP and EmfA transporters [102,103].

Plants

Previously introduced Mn^{2+} transporters also involved in iron homeostasis in plants include: YSL importers (PM, chloroplast, vacuole, ER) [25,104]; Nramp importers (PM, chloroplast, vacuole) [47,104,105]; importer IRT1 (PM) [24,105]; and VIT1 exporting Fe^{2+} into the vacuole [25,105]; (Figure 5B, Table 3). In addition, ABC transporter ATM3 exports iron from the mitochondria [24,105,106] and ABC transporter IDI7 imports Fe^{2+} from the vacuole into cytosol [47,107]; MFS-family FPN2 [105,108] and ZIP-family IRT2 [47,105,109] export Fe^{2+} from cytosol into vacuoles; and the PIC1 permease imports Fe^{2+} into the chloroplast stroma [25,105] (Figure 5B, Table 3).

Fungi

As with Mn^{2+}, the fungal iron homeostasis machinery is best understood in yeasts (Figure 5C, Table 3). Key importers include: permeases Ftr1/Fip1 (PM) and Fth1/Ftr2 (vacuole) import Fe^{3+} [2,110]; permease Fet4 imports Fe^{2+} [2,94]; Nramp-family Smf1 (PM) and Smf3 (vacuole) import Fe^{2+} [2,34,94]; MFS-family Str3 (PM), heme receptor Shu1 (PM), ABC transporter Abc3 (vacuole), all import heme [110]; MFS-family Arn1-4, Sit1, Str1, Ernb1 Taf1 import Fe^{3+}-siderophores across the PM [94,110-112].CCC1-family Ccc1 and Pcl1 export Fe^{2+} into vacuoles [2,110,113]. Finally, mitochondrial carrier (MC)-family Mrs3/4 import Fe^{2+} into the mitochondrial matrix [2,114,115].

Animals

Iron homeostasis in animals has many players that enable fluxes of free iron ions and iron complexes like Fe^{2+}-heme and Fe-S clusters (Figure 5D and Table 3). Here we focus on proteins with major roles in transporting non-heme iron. In animals, iron primarily circulates as Fe^{3+}-transferrin, which captured at the cell surface by TfR1/2 and internalized into endosomes [28,65,116]. Fe^{3+} from transferrin and other endocytosed complexes is released in acidic endosomes, converted to Fe^{2+} by reductases like STEAP3, and Fe^{2+} is then imported by NRAMP2 into the cytosol [21,34,116]. Cytosolic Fe^{2+} is either taken up in the mitochondria by MC-family MFRN1/2 for Fe-S cluster biogenesis and energy production, stored in ferritin for future use, or exported across the PM by ferroportin [17,101,117]. Additional Fe^{2+} importers include: ZIP8/14 (PM) [28]; the Ca^{2+} channel LTCC (PM) [28,118]; and the non-selective cation channel TRPML1 (endosomes and lysosome) [119,120].

Iron is central to the antimicrobial and erythrophagocytosis activities of macrophages. The iron transporters in macrophage cells are a subset of a regular animal cell, with the important addition of NRAMP1 at the phagosomal membrane that plays a key role in nutritional

immunity, depriving phagocytosed pathogens of Fe^{2+} as it does for Mn^{2+} (Figure 5E) [34,121].

Structural insights into iron binding and transport

Iron is transported across membranes either as ions (Fe^{2+}/Fe^{3+}) or bound to heme or chelators like siderophores [65,122,123]. For these iron complexes, iron remains tightly bound to the respective chelator through the membrane transport process. In contrast, ionic forms of iron need to interact transiently with their transporters to enable rapid cycles of binding and release. Both Fe^{2+} and Fe^{3+} prefer octahedral geometry, with optimal bond lengths of 2.0-2.5 Å, although 'weak interactions' of 2.5-3.0 Å can still participate in a coordination sphere [78,80,85]. Here, we compare the coordination geometry and binding affinity of different iron binding sites, including ionic and complexed forms, to understand whether these properties help explain the distinct physiological functions of different transporters.

Siderophores, Heme and Transferrin

Structures of iron chelator complexes reveal near-ideal coordination geometry, consistent with their extremely high affinity for iron (Figure 6, Table 4). For example, the vibriobactin siderophore and heme (with contributions of the heme receptor protein PhuT) coordinate Fe^{3+} and Fe^{2+}, respectively, octahedrally with optimal bond lengths and minimal angular deviation (Figure 6A-B, Table 4) [124-127]. Most siderophores are hexadentate and do not require additional interacting residues from the host proteins to complete Fe^{3+}-octahedral coordination. An exception is tetradentate unsaturated siderophores captured by the periplasmic binding protein CeuE from *Campylobacter jejuni*. CeuE uses a histidine and a tyrosine to complete the near-ideal coordination of Fe^{3+} [128] (Table 4). Human transferrin—which mediates circulation of the poorly soluble Fe^{3+} in blood plasma while limiting levels of free Fe^{3+}—binds Fe^{3+} with very high affinity ($K_d \sim 10^{-21}$ M) [129]. Correspondingly, the Fe^{3+}-transferrin also has near-perfect octahedral coordination geometry (Figure 6C, Table 4) [130]. According to the HSAB (hard and soft acid and base) theory, Fe^{3+} is a hard ion, and its ideal coordination sphere contains mostly hard oxygen ligands (with one nitrogen in both Fe^{3+} complexes illustrated in Figure 6). In contrast, Fe^{2+}, a softer metal ion, and a heme provides four nitrogen ligands—with nitrogen being a softer ligand than oxygen.

Metal-binding domains of transporters

VIT1 (vacuolar iron transporter 1), is primarily involved in iron export into vacuoles of plant and fungal cells, although it also transports other transition metals including Co^{2+}, Zn^{2+}, Mn^{2+} [49]. VIT1 has a cytosolic metal-binding domain (MBD) that is thought to capture iron before its eventual transfer to the transmembrane transport domain. A structure of the *Eucalyptus grandis* VIT1 MBD shows Fe^{2+} bound in a near-ideal octahedral coordination (Figure 6D, Table 4) [50]. However, the 4-Å bond to M149—a residue essential for metal transport—is longer than expected for a strong bonding interaction. Consistent with this observation, a K_d value of 1.9 ± 0.4 μM for Fe^{2+} binding to full-length VIT1 [49] suggests

that none of its Fe^{2+}-binding sites are as ideal as those of the chelators and binding proteins described above.

The SBPs of iron-specific ABC transporters also trap iron before transferring it to the transport module [131], and the iron binding geometry and affinity reveal a similar trend as that of VIT1. A representative SBP (YfeA, SBP of the iron importer YfeABC from *Yersinia pestis*) binds Fe^{3+} in its preferred octahedral coordination, but with angular distortions and some longer bond lengths (Figure 6E, Table 4) [132]. Again, similarly to VIT1, YfeA and MtsA (a Fe^{2+} SBP from *Streptococcus pyogenes*) have metal-binding affinities in the nM to low μM range (Table 4) [133,134].

Ferroportin

The bacterial ferroportin homolog *Bdellovibrio bacteriovorus* (Bb)FPN is the only protein for which we have a high-resolution structure with iron bound in the transmembrane transport domain. A structure of human ferroportin (FPN) bound to Co^{2+} provides clues of its Fe^{2+} binding and transport mechanism [135]. However, in absence of Fe^{2+}-bound structures, we do not further discuss the human FPN structure. In BpFPN, Fe^{2+} binds in a non-ideal trigonal bipyramidal geometry with a high angular deviation and all coordinating bond lengths are longer than ideal (Figure 6F, Table 4). Moreover, BbFPN binds Co^{2+} (a transported substrate similar to, but more stable in solution, than Fe^{2+}) with a K_d of 195 μM [41,77]. This affinity is similar to that observed for DraNramp and Mn^{2+}. Mfrn1 from *Oreochromis niloticus*, another Fe^{2+} transporter, also display low affinity (K_d of 450 μM for Fe^{2+}) [72]. Imperfect coordination geometry (bond angles and lengths) and poor binding affinity may be instrumental for ensuring conformational transitions and metal mobility required for transport.

Conclusions

The available Mn^{2+} transporter structures reveal that diverse coordination geometry and ligand type can enable Mn^{2+} binding and transport. Furthermore, distinct binding site structures result in different mechanisms for selectivity. Interestingly, in different Mn^{2+} transporters, either deviations from ideal bonding geometry or number of coordinating ligands allow both Mn^{2+} release and conformational changes seem to be required for transport to be kinetically accessible.

Similarly, analyses of the iron binders, chelators, and transporters show how both the ion binding properties and affinity correlate with the biological role of each type of iron interaction, with the binders (chelators and transferrin) having near-ideal coordination and much higher affinity towards iron compared to the transporters like BbFPN, and binding domains of transporters (SBPs and the VIT1 MBD), falling somewhere in between binders and canonical transporters.

Another general observation is that when comparing the binding of different metals to the same protein, affinity often poorly correlates with how ideal the coordination geometry is. This suggests that other energetic contributions are at play, such as conformational changes of the protein to accommodate the metal. Binding of a metal ion may cause a conformational

change in the protein that incurs an energetic penalty, affecting the overall affinity of the protein for the metal. Furthermore, this conformational change may be on- or off-pathway in terms of the physiological function of the protein. For example, in DraNramp, the protein binds Mn^{2+} in a closer-to-ideal geometry than Cd^{2+} does, but that seems to come with some energetic cost because its affinity for Mn^{2+} is lower than that for Cd^{2+}. In the case of PsaA, binding of Zn^{2+} is high affinity, but Zn^{2+} is not transported by PsaABC, presumably because the resulting PsaABC structure is not conducive to the next conformational steps in the transport cycle.

Overall, this review highlights how atomic-level knowledge of the coordination chemistry of different transition metals can help us understand the function of proteins in Mn^{2+} and iron homeostasis and how the transport behavior of the proteins may change during dyshomeostatic conditions.

Acknowledgements

We thank members of the Gaudet lab for discussion and feedback. This work was funded by NIGMS grant R01GM120996 (R.G.).

References

1. Pajarillo EAB, Lee E, Kang D-K (2021) Trace metals and animal health: Interplay of the gut microbiota with iron, manganese, zinc, and copper. Anim. Nutr 7, 750–61 10.1016/j.aninu.2021.03.005 [PubMed: 34466679]
2. Bleackley MR, MacGillivray RTA (2011) Transition metal homeostasis: from yeast to human disease. Biometals. 24, 785–809 10.1007/s10534-011-9451-4 [PubMed: 21479832]
3. Chen P, Bornhorst J, Aschner MA (2018) Manganese metabolism in humans. Front. Biosci 23(9), 1655–1679 10.2741/4665
4. Candas D, Li JJ (2013) MnSOD in Oxidative Stress Response-Potential Regulation via Mitochondrial Protein Influx. Antioxid. Redox Signal 20, 1599–617 10.1089/ars.2013.5305 [PubMed: 23581847]
5. Studer JM, Schweer WP, Gabler NK, Ross JW (2022) Functions of manganese in reproduction. Anim. Reprod. Sci 106924 10.1016/j.anireprosci.2022.106924 [PubMed: 35121412]
6. Budinger D, Barral S, Soo AKS, Kurian MA (2021) The role of manganese dysregulation in neurological disease: emerging evidence. Lancet Neurol. 20, 956–68 10.1016/S1474-4422(21)00238-6 [PubMed: 34687639]
7. Chen P, Chakraborty S, Mukhopadhyay S, Lee E, Paoliello MM, Bowman AB, et al. (2015) Manganese homeostasis in the nervous system. J Neurochem. 134, 601–10 10.1111/jnc.13170 [PubMed: 25982296]
8. Harischandra DS, Ghaisas S, Zenitsky G, Jin H, Kanthasamy A, Anantharam V, et al. (2019) Manganese-Induced Neurotoxicity: New Insights Into the Triad of Protein Misfolding, Mitochondrial Impairment, and Neuroinflammation. Front. Neurosci 13 10.3389/fnins.2019.00654
9. Socha A, Guerinot ML (2014) Mn-euvering manganese: the role of transporter gene family members in manganese uptake and mobilization in plants. Front. Plant Sci 5. 10.3389/fpls.2014.00106
10. Devanna BN, Jaswal R, Singh PK, Kapoor R, Jain P, Kumar G, et al. (2021) Role of transporters in plant disease resistance. Physiol. Plant 171, 849–67 10.1111/ppl.13377 [PubMed: 33639002]
11. Li J, Jia Y, Dong R, Huang R, Liu P, Li X, et al. (2019) Advances in the Mechanisms of Plant Tolerance to Manganese Toxicity. Int. J. Mol. Sci 20 10.3390/ijms20205096
12. Waters LS (2020) Bacterial manganese sensing and homeostasis. Curr. Opin. Chem. Biol 55, 96–102 10.1016/j.cbpa.2020.01.003 [PubMed: 32086169]

13. Bosma EF, Rau MH, van Gijtenbeek LA, Siedler S (2021) Regulation and distinct physiological roles of manganese in bacteria. FEMS Microbiol. Rev 45 10.1093/femsre/fuab028
14. Abreu IA, Cabelli DE (2010) Superoxide dismutases—a review of the metal-associated mechanistic variations. Biochim Biophys Acta Proteins Proteom. 1804, 263–74 10.1016/j.bbapap.2009.11.005
15. Guo S, Frazer DM, Anderson GJ (2016) Iron homeostasis: transport, metabolism, and regulation. Curr. Opin. Clin. Nutr. Metab. Care 19, 276–81 10.1097/mco.0000000000000285 [PubMed: 27137899]
16. Knutson MD (2017) Iron transport proteins: Gateways of cellular and systemic iron homeostasis. J. Biol. Chem 292, 12735–43 10.1074/jbc.R117.786632 [PubMed: 28615441]
17. Liu Q, Wu J, Zhang X, Wu X, Zhao Y, Ren J (2021) Iron homeostasis and disorders revisited in the sepsis. Free Rad. Biol. Med 165, 1–13 10.1016/j.freeradbiomed.2021.01.025 [PubMed: 33486088]
18. Peace JM, Banayan JM (2021) Anemia in pregnancy: pathophysiology, diagnosis, and treatment. Int. Anesthesiol. Clin 59, 15–21 10.1097/aia.0000000000000320
19. Naito Y, Masuyama T, Ishihara M (2021) Iron and cardiovascular diseases. J. Cardiol 77, 160–5 10.3390/2Fph12030125 [PubMed: 32739111]
20. Rana S, Prabhakar N (2021) Iron disorders and hepcidin. Clin. Chim. Acta 523, 454–68 10.1016/j.cca.2021.10.032 [PubMed: 34755647]
21. Zeidan RS, Han SM, Leeuwenburgh C, Xiao R (2021) Iron homeostasis and organismal aging. Ageing Res. Rev 72, 101510 10.1016/j.arr.2021.101510 [PubMed: 34767974]
22. Koleini N, Shapiro JS, Geier J, Ardehali H (2021) Ironing out mechanisms of iron homeostasis and disorders of iron deficiency. J. Clin. Investig 131 10.1172/jci148671
23. Pilon M, Cohu CM, Ravet K, Abdel-Ghany SE, Gaymard F (2009) Essential transition metal homeostasis in plants. Curr. Opin. Plant Biol 12, 347–57 10.1016/j.pbi.2009.04.011 [PubMed: 19481497]
24. Connorton JM, Balk J, Rodríguez-Celma J (2017) Iron homeostasis in plants - a brief overview. Metallomics 9, 813–23 10.1039/c7mt00136c [PubMed: 28686269]
25. Kroh GE, Pilon M (2020) Regulation of iron homeostasis and use in chloroplasts. Int. J. Mol. Sci 21, 3395 10.3390/ijms21093395 [PubMed: 32403383]
26. Zhang X, Zhang D, Sun W, Wang T (2019) The Adaptive Mechanism of Plants to Iron Deficiency via Iron Uptake, Transport, and Homeostasis. Int. J. Mol. Sci 20 10.3390/ijms20102424
27. Ma Z, Jacobsen FE, Giedroc DP (2009) Coordination Chemistry of Bacterial Metal Transport and Sensing. Chem. Rev 109, 4644–81 10.1021/cr900077w [PubMed: 19788177]
28. Liu Q, Barker S, Knutson MD (2021) Iron and manganese transport in mammalian systems. Biochim. Biophys. Acta Mol. Cell Res 1868, 118890 10.1016/j.bbamcr.2020.118890 [PubMed: 33091506]
29. Krewulak KD, Vogel HJ (2008) Structural biology of bacterial iron uptake. Biochim. Biophys. Acta Biomembr 1778, 1781–804 10.1016/j.bbamem.2007.07.026
30. Rulísek L, Vondrásek J (1998) Coordination geometries of selected transition metal ions (Co^{2+}, Ni^{2+}, Cu^{2+}, Zn^{2+}, Cd^{2+}, and Hg^{2+}) in metalloproteins. J. Inorg. Biochem 71, 115–27 10.1016/s0162-0134(98)10042-9 [PubMed: 9833317]
31. Couñago RM, Ween MP, Begg SL, Bajaj M, Zuegg J, O'Mara ML, et al. (2014) Imperfect coordination chemistry facilitates metal ion release in the Psa permease. Nature Chem. Biol 10, 35–41 10.1038/nchembio.1382 [PubMed: 24212134]
32. Foster AW, Osman D, Robinson NJ (2014) Metal Preferences and Metallation. J. Biol. Chem 289, 28095–103 10.1074/jbc.r114.588145 [PubMed: 25160626]
33. Klein JS, Lewinson O (2011) Bacterial ATP-driven transporters of transition metals: physiological roles, mechanisms of action, and roles in bacterial virulence. Metallomics. 3 10.1039/c1mt00073j
34. Bozzi AT, Gaudet R (2021) Molecular Mechanism of Nramp-Family Transition Metal Transport. J. Mol. Biol 433, 166991. 10.1016/j.jmb.2021.166991 [PubMed: 33865868]
35. Hohle Thomas H, Franck William L, Stacey G, O'Brian Mark R (2011) Bacterial outer membrane channel for divalent metal ion acquisition. Proc. Natl. Acad. Sci. U. S. A 108, 15390–5. 10.1073/pnas.1110137108 [PubMed: 21880957]

36. Raimunda D, Elso-Berberián G (2014) Functional characterization of the CDF transporter SMc02724 (SmYiiP) in Sinorhizobium meliloti: Roles in manganese homeostasis and nodulation. Biochim. Biophys. Acta Biomembr 1838, 3203–11 10.1016/j.bbamem.2014.09.005
37. Ouyang A, Gasner Kendall M, Neville Stephanie L, McDevitt Christopher A, Frawley Elaine R (2022) MntP and YiiP Contribute to Manganese Efflux in Salmonella enterica Serovar Typhimurium under Conditions of Manganese Overload and Nitrosative Stress. Microbiol. Spectr 10, e01316–21. 10.1128/spectrum.01316-21 [PubMed: 35019706]
38. Paruthiyil S, Pinochet-Barros A, Huang X, Helmann JD (2020) Bacillus subtilis TerC Family Proteins Help Prevent Manganese Intoxication. J. Bacteriol 202 10.1128/jb.00624-19
39. Wu Q, Mu Q, Xia Z, Min J, Wang F (2021) Manganese homeostasis at the host-pathogen interface and in the host immune system. Semin. Cell Dev. Biol 115, 45–53 10.1016/j.semcdb.2020.12.006 [PubMed: 33419608]
40. Ha N, Lee EJ (2023) Manganese Transporter Proteins in *Salmonella enterica serovar Typhimurium*. J. Microbiol 61, 289–296 10.1007/s12275-023-00027-7 [PubMed: 36862278]
41. Taniguchi R, Kato HE, Font J, Deshpande CN, Wada M, Ito K, et al. (2015) Outward- and inward-facing structures of a putative bacterial transition-metal transporter with homology to ferroportin. Nat. Commun 6, 8545 10.1038/ncomms9545 [PubMed: 26461048]
42. Martin JE, Le MT, Bhattarai N, Capdevila DA, Shen J, Winkler ME, et al. (2019) A Mn-sensing riboswitch activates expression of a Mn^{2+}/Ca^{2+} ATPase transporter in Streptococcus. Nucleic Acids Res. 47, 6885–99 10.1093/nar/gkz494 [PubMed: 31165873]
43. Waters LS, Sandoval M, Storz G (2011) The Escherichia coli MntR miniregulon includes genes encoding a small protein and an efflux pump required for manganese homeostasis. J. Bacteriol 193, 5887–97. 10.1128/jb.05872-11 [PubMed: 21908668]
44. Lubkowitz M (2006) The OPT family functions in long-distance peptide and metal transport in plants. Genet. Engg 27, 35–55 10.1007/0-387-25856-6_3
45. Milner MJ, Seamon J, Craft E, Kochian LV (2013) Transport properties of members of the ZIP family in plants and their role in Zn and Mn homeostasis. J. Exp. Bot 64, 369–81 10.1093/jxb/ers315 [PubMed: 23264639]
46. Shigaki T, Pittman JK, Hirschi KD (2003) Manganese specificity determinants in the Arabidopsis metal/H+ antiporter CAX2. J. Biol. Chem 278, 6610–7 10.1074/jbc.m209952200 [PubMed: 12496310]
47. Hall JL, Williams LE (2003) Transition metal transporters in plants. J. Exp. Bot 54, 2601–13 10.1093/jxb/erg303 [PubMed: 14585824]
48. Connorton JM, Jones ER, Rodríguez-Ramiro I, Fairweather-Tait S, Uauy C, Balk J (2017) Wheat Vacuolar Iron Transporter TaVIT2 Transports Fe and Mn and Is Effective for Biofortification. Plant Physiol. 174, 2434–44 10.1104/pp.17.00672 [PubMed: 28684433]
49. Labarbuta P, Duckett K, Botting CH, Chahrour O, Malone J, Dalton JP, et al. (2017) Recombinant vacuolar iron transporter family homologue PfVIT from human malaria-causing Plasmodium falciparum is a Fe^{2+}/H^{+} exchanger. Sci. Rep 7, 42850 10.1038/srep42850 [PubMed: 28198449]
50. Kato T, Kumazaki K, Wada M, Taniguchi R, Nakane T, Yamashita K, et al. (2019) Crystal structure of plant vacuolar iron transporter VIT1. Nat. Plants 5, 308–15 10.1038/s41477-019-0367-2 [PubMed: 30742036]
51. Thines L, Deschamps A, Stribny J, Morsomme P (2019) Yeast as a Tool for Deeper Understanding of Human Manganese-Related Diseases. Genes 10 10.3390/genes10070545
52. Culotta Valeria C, Yang M, Hall Matthew D (2005) Manganese Transport and Trafficking: Lessons Learned from *Saccharomyces cerevisiae*. Eukaryot. Cell 4, 1159–65 10.1128/EC.4.7.1159-1165.2005 [PubMed: 16002642]
53. Pittman JK (2005) Managing the manganese: molecular mechanisms of manganese transport and homeostasis. New Phytol. 167, 733–42 10.1111/j.1469-8137.2005.01453.x [PubMed: 16101910]
54. Reddi AR, Jensen LT, Culotta VC (2009) Manganese homeostasis in *Saccharomyces cerevisiae*. Chem. Rev 109, 4722–32 10.1021/cr900031u [PubMed: 19705825]
55. Andreeva N, Kulakovskaya E, Zvonarev A, Penin A, Eliseeva I, Teterina A, et al. (2017) Transcriptome profile of yeast reveals the essential role of PMA2 and uncharacterized gene

YBR056W-A (MNC1) in adaptation to toxic manganese concentration. Metallomics. 9, 175–82 10.1039/c6mt00210b [PubMed: 28128390]

56. Jensen LT, Ajua-Alemanji M, Culotta VC (2003) The *Saccharomyces cerevisiae* high affinity phosphate transporter encoded by PHO84 also functions in manganese homeostasis. J Biol Chem. 278, 42036–40 10.1074/jbc.m307413200 [PubMed: 12923174]
57. Lin SJ, Culotta VC (1996) Suppression of oxidative damage by *Saccharomyces cerevisiae* ATX2, which encodes a manganese-trafficking protein that localizes to Golgi-like vesicles. Mol. Cell. Biol 16, 6303–12 10.1128/mcb.16.11.6303 [PubMed: 8887660]
58. García-Rodríguez N, Manzano-López J, Muñoz-Bravo M, Fernández-García E, Muñiz M, Wellinger RE (2015) Manganese redistribution by calcium-stimulated vesicle trafficking bypasses the need for P-type ATPase function. J. Biol. Chem 290, 9335–47 10.1074/jbc.m114.616334 [PubMed: 25713143]
59. Chesi A, Kilaru A, Fang X, Cooper AA, Gitler AD (2012) The role of the Parkinson's disease gene PARK9 in essential cellular pathways and the manganese homeostasis network in yeast. PLoS One. 7, e34178 10.1371/journal.pone.0034178 [PubMed: 22457822]
60. Potelle S, Dulary E, Climer L, Duvet S, Morelle W, Vicogne D, et al. (2017) Manganese-induced turnover of TMEM165. Biochem. J 474, 1481–93 10.1042/bcj20160910 [PubMed: 28270545]
61. Thines L, Deschamps A, Sengottaiyan P, Savel O, Stribny J, Morsomme P (2018) The yeast protein Gdt1p transports Mn2+ ions and thereby regulates manganese homeostasis in the Golgi. J. Biol. Chem 293, 8048–55 10.1074/jbc.RA118.002324 [PubMed: 29632074]
62. Luk E, Carroll M, Baker M, Culotta VC (2003) Manganese activation of superoxide dismutase 2 in *Saccharomyces cerevisiae* requires MTM1, a member of the mitochondrial carrier family. Proc. Natl. Acad. Sci. U. S. A 100, 10353–7 10.1073/pnas.1632471100 [PubMed: 12890866]
63. Lisher J, Giedroc D (2013) Manganese acquisition and homeostasis at the host-pathogen interface. Front. Cell. Infect. Microbiol 3 10.3389/fcimb.2013.00091
64. Herrera C, Pettiglio MA, Bartnikas TB (2014) Investigating the role of transferrin in the distribution of iron, manganese, copper, and zinc. J. Biol. Inorg. Chem 19, 869–77 10.1007/s00775-014-1118-5 [PubMed: 24567067]
65. Kawabata H (2019) Transferrin and transferrin receptors update. Free Radic. Biol. Med 133, 46–54 10.1016/j.freeradbiomed.2018.06.037 [PubMed: 29969719]
66. Au C, Benedetto A, Aschner M (2008) Manganese transport in eukaryotes: the role of DMT1. Neurotoxicology 29, 569–76 10.1016/j.neuro.2008.04.022 [PubMed: 18565586]
67. Fujishiro H, Kambe T (2022) Manganese transport in mammals by zinc transporter family proteins, ZNT and ZIP. J. Pharmacol. Sci 148, 125–33 10.1016/j.jphs.2021.10.011 [PubMed: 34924116]
68. Sigel A, Sigel H, Sigel RK (2014) Interrelations between essential metal ions and human diseases. Metal ions in life sciences. Transit. Met. Chem 39, 971–972 10.1007/978-94-007-7500-8
69. Fleming SM, Santiago NA, Mullin EJ, Pamphile S, Karkare S, Lemkuhl A, et al. (2018) The effect of manganese exposure in Atp13a2-deficient mice. NeuroToxicology. 64, 256–66 10.1016/j.neuro.2017.06.005 [PubMed: 28595912]
70. Grice DM, Vetter I, Faddy HM, Kenny PA, Roberts-Thomson SJ, Monteith GR (2010) Golgi Calcium Pump Secretory Pathway Calcium ATPase 1 (SPCA1) Is a Key Regulator of Insulin-like Growth Factor Receptor (IGF1R) Processing in the Basal-like Breast Cancer Cell Line MDA-MB-231. J. Biol. Chem 285, 37458–66 10.1074/jbc.m110.163329 [PubMed: 20837466]
71. Takeda A (2003) Manganese action in brain function. Brain Res. Rev 41, 79–87. 10.1016/S0165-0173(02)00234-5 [PubMed: 12505649]
72. Christenson ET, Gallegos AS, Banerjee A (2018) In vitro reconstitution, functional dissection, and mutational analysis of metal ion transport by mitoferrin-1. J. Biol. Chem 293, 3819–28 10.1074/jbc.m117.817478 [PubMed: 29305420]
73. Horning KJ, Caito SW, Tipps KG, Bowman AB, Aschner M (2015) Manganese Is Essential for Neuronal Health. Annu. Rev. Nutr 35, 71–108 10.1146/annurev-nutr-071714-034419 [PubMed: 25974698]
74. Lawrence MC, Pilling PA, Epa VC, Berry AM, Ogunniyi AD, Paton JC (1998) The crystal structure of pneumococcal surface antigen PsaA reveals a metal-binding site and a novel structure

for a putative ABC-type binding protein. Structure 6, 1553–61 10.1016/S0969-2126(98)00153-1 [PubMed: 9862808]

75. Abate F, Malito E, Cozzi R, Lo Surdo P, Maione D, Bottomley MJ (2014) Apo, Zn^{2+}-bound and Mn^{2+}-bound structures reveal ligand-binding properties of SitA from the pathogen *Staphylococcus pseudintermedius*. Biosci. Rep 34, e00154 10.1042/BSR20140088 [PubMed: 25311310]
76. Bozzi AT, Zimanyi CM, Nicoludis JM, Lee BK, Zhang CH, Gaudet R (2019) Structures in multiple conformations reveal distinct transition metal and proton pathways in an Nramp transporter. Elife 8, e41124 10.7554/eLife.41124 [PubMed: 30714568]
77. Pan Y, Ren Z, Gao S, Shen J, Wang L, Xu Z, et al. (2020) Structural basis of ion transport and inhibition in ferroportin. Nat. Commun 11, 5686 10.1038/s41467-020-19458-6 [PubMed: 33173040]
78. Harding M. (2000) The geometry of metal-ligand interactions relevant to proteins. II. Angles at the metal atom, additional weak metal-donor interactions. Acta Crystallogr. D. Biol. Crystallogr 56, 857–67. 10.1107/s0907444900005849 [PubMed: 10930832]
79. Harding M. (2001) Geometry of metal-ligand interactions in proteins. Acta Crystallogr. D. Biol. Crystallogr 57, 401–11 10.1107/s0907444900019168 [PubMed: 11223517]
80. Harding M (2006) Small revisions to predicted distances around metal sites in proteins. Acta Crystallogr. D. Biol. Crystallogr 62, 678–82 10.1107/s0907444906014594 [PubMed: 16699196]
81. Ray S, Berry SP, Wilson EA, Zhang CH, Shekhar M, Singharoy A, et al. (2023) High-resolution structures with bound Mn^{2+} and Cd^{2+} map the metal import pathway in an Nramp transporter. eLife. 12, e84006 10.7554/eLife.84006 [PubMed: 37039477]
82. Golynskiy MV, Gunderson WA, Hendrich MP, Cohen SM (2006) Metal Binding Studies and EPR Spectroscopy of the Manganese Transport Regulator MntR. Biochemistry 45, 15359–72 10.1021/bi0607406 [PubMed: 17176058]
83. Kliegman JI, Griner SL, Helmann JD, Brennan RG, Glasfeld A (2006) Structural basis for the metal-selective activation of the manganese transport regulator of *Bacillus subtilis*. Biochemistry 45, 3493–505 10.1021/bi0524215 [PubMed: 16533030]
84. Glasfeld A, Guedon E, Helmann JD, Brennan RG (2003) Structure of the manganese-bound manganese transport regulator of *Bacillus subtilis*. Nat. Struct. Biol 10, 652–7 10.1038/nsb951 [PubMed: 12847518]
85. Zheng H, Chruszcz M, Lasota P, Lebioda L, Minor W (2008) Data mining of metal ion environments present in protein structures. J. Inorg. Biochem 102, 1765–76 10.1016/j.jinorgbio.2008.05.006 [PubMed: 18614239]
86. Neville SL, Sjöhamn J, Watts JA, MacDermott-Opeskin H, Fairweather SJ, Ganio K, et al. (2021) The structural basis of bacterial manganese import. Sci. Adv 7. 10.1126/sciadv.abg3980
87. McDevitt CA, Ogunniyi AD, Valkov E, Lawrence MC, Kobe B, McEwan AG, et al. (2011) A Molecular Mechanism for Bacterial Susceptibility to Zinc. PLOS Pathog. 7, e1002357 10.1371/journal.ppat.1002357 [PubMed: 22072971]
88. Jacobsen FE, Kazmierczak KM, Lisher JP, Winkler ME, Giedroc DP (2011) Interplay between manganese and zinc homeostasis in the human pathogen *Streptococcus pneumoniae*. Metallomics. 3, 38–41 10.1039/c0mt00050g [PubMed: 21275153]
89. Rukhman V, Anati R, Melamed-Frank M, Adir N (2005) The MntC Crystal Structure Suggests that Import of Mn^{2+} in Cyanobacteria is Redox Controlled. J. Mol. Biol 348, 961–9 10.1016/j.jmb.2005.03.006 [PubMed: 15843026]
90. Chen J, Smaardijk S, Mattelaer C-A, Pamula F, Vandecaetsbeek I, Vanoevelen J, et al. (2019) An N-terminal Ca^{2+}-binding motif regulates the secretory pathway Ca^{2+}/Mn^{2+}-transport ATPase SPCA1. J. Biol. Chem 294, 7878–91 10.1074/jbc.RA118.006250 [PubMed: 30923126]
91. Chen Z, Watanabe S, Hashida H, Inoue M, Daigaku Y, Kikkawa M, et al. Cryo-EM structures of human SPCA1a reveal the mechanism of Ca^{2+}/Mn^{2+} transport into the Golgi apparatus. Sci. Adv 9, eadd9742 10.1126/sciadv.add9742
92. Xue J, Xie T, Zeng W, Jiang Y, Bai XC (2020) Cryo-EM structures of human ZnT8 in both outward- and inward-facing conformations. Elife. 9, e58823 10.7554/eLife.58823 [PubMed: 32723473]

93. Zhang T, Liu J, Fellner M, Zhang C, Sui D, Hu J (2017) Crystal structures of a ZIP zinc transporter reveal a binuclear metal center in the transport pathway. Sci. Adv 3, e1700344 10.1126/sciadv.1700344 [PubMed: 28875161]
94. Banci L, Bertini I. (2013) Metallomics and the cell: some definitions and general comments. Met. Ions Life Sci 12, 1–13 10.1007/978-94-007-5561-1_1 [PubMed: 23595668]
95. Hood MI, Skaar EP (2012) Nutritional immunity: transition metals at the pathogen–host interface. Nature Rev. Microbiol 10, 525–37 10.1038/nrmicro2836 [PubMed: 22796883]
96. Klebba PE, Newton SMC, Six DA, Kumar A, Yang T, Nairn BL, et al. (2021) Iron Acquisition Systems of Gram-negative Bacterial Pathogens Define TonB-Dependent Pathways to Novel Antibiotics. Chem. Rev 121, 5193–239 10.1021/acs.chemrev.0c01005 [PubMed: 33724814]
97. Garmory Helen S, Titball Richard W (2004) ATP-Binding Cassette Transporters Are Targets for the Development of Antibacterial Vaccines and Therapies. Infect. Immun 72, 6757–63 10.1128/IAI.72.12.6757-6763.2004 [PubMed: 15557595]
98. Marlovits TC, Haase W, Herrmann C, Aller SG, Unger VM (2002) The membrane protein FeoB contains an intramolecular G protein essential for Fe (II) uptake in bacteria. Proc. Nat. Acad. Sci. U.S.A 99, 16243–8 10.1073/pnas.242338299
99. Hung KW, Chang YW, Eng ET, Chen JH, Chen YC, Sun YJ, et al. (2010) Structural fold, conservation and Fe(II) binding of the intracellular domain of prokaryote FeoB. J Struct. Biol 170, 501–12 10.1016/j.jsb.2010.01.017 [PubMed: 20123128]
100. Drakesmith H, Nemeth E, Ganz T (2015) Ironing out Ferroportin. Cell Metab. 22, 777–87 10.1016/j.cmet.2015.09.006 [PubMed: 26437604]
101. Gammella E, Correnti M, Cairo G, Recalcati S (2021) Iron Availability in Tissue Microenvironment: The Key Role of Ferroportin. Int. J. Mol. Sci 22(6), 2986 10.3390/ijms22062986 [PubMed: 33804198]
102. Grass G, Otto M, Fricke B, Haney CJ, Rensing C, Nies DH, et al. (2005) FieF (YiiP) from Escherichia coli mediates decreased cellular accumulation of iron and relieves iron stress. Arch. Microbiol 183, 9–18 10.1007/s00203-004-0739-4 [PubMed: 15549269]
103. Cubillas C, Vinuesa P, Luisa Tabche M, Dávalos A, Vázquez A, Hernández-Lucas I, et al. (2014) The cation diffusion facilitator protein EmfA of Rhizobium etli belongs to a novel subfamily of Mn^{2+}/Fe^{2+} transporters conserved in α-proteobacteria. Metallomics 6, 1808–15 10.1039/c4mt00135d [PubMed: 25054342]
104. Krämer U, Talke IN, Hanikenne M (2007) Transition metal transport. FEBS Lett. 581, 2263–72 10.1016/j.febslet.2007.04.010 [PubMed: 17462635]
105. Agafonov O, Selstø CH, Thorsen K, Xu XM, Drengstig T, Ruoff P (2016) The organization of controller motifs leading to robust plant iron homeostasis. PloS one. 11, e0147120 10.1371/journal.pone.0147120 [PubMed: 26800438]
106. Balk J, Lobréaux S (2005) Biogenesis of iron–sulfur proteins in plants. Trends Plant Sci. 10, 324–31 10.1016/j.tplants.2005.05.002 [PubMed: 15951221]
107. Yamaguchi H, Nishizawa NK, Nakanishi H, Mori S (2002) IDI7, a new iron-regulated ABC transporter from barley roots, localizes to the tonoplast. J. Exp. Bot 53, 727–35 10.1093/jexbot/53.369.727 [PubMed: 11886893]
108. Morrissey J, Baxter IR, Lee J, Li L, Lahner B, Grotz N, et al. (2009) The Ferroportin Metal Efflux Proteins Function in Iron and Cobalt Homeostasis in Arabidopsis. Plant Cell 21, 3326–38 10.1105/tpc.109.069401 [PubMed: 19861554]
109. Clemens S (2001) Molecular mechanisms of plant metal tolerance and homeostasis. Planta. 212, 475–86 10.1007/s004250000458 [PubMed: 11525504]
110. Martínez-Pastor MT, Puig S (2020) Adaptation to iron deficiency in human pathogenic fungi. Biochim. Biophys. Acta Mol. Cell. Res 1867, 118797 10.1016/j.bbamcr.2020.118797 [PubMed: 32663505]
111. Lesuisse E, Blaiseau P-L, Dancis A, Camadro J-M (2001) Siderophore uptake and use by the yeast Saccharomyces cerevisiae. Microbiology. 147, 289–98 10.1099/00221287-147-2-289 [PubMed: 11158346]

112. Kim Y, Lampert SM, Philpott CC (2005) A receptor domain controls the intracellular sorting of the ferrichrome transporter, ARN1. EMBO J. 24, 952–62 10.1038/sj.emboj.7600579 [PubMed: 15719020]
113. Robinson JR, Isikhuemhen OS, Anike FN (2021) Fungal-Metal Interactions: A Review of Toxicity and Homeostasis. J. Fungi 7(3), 225 10.3390/jof7030225
114. Mühlenhoff U, Stadler JA, Richhardt N, Seubert A, Eickhorst T, Schweyen RJ, et al. (2003) A specific role of the yeast mitochondrial carriers MRS3/4p in mitochondrial iron acquisition under iron-limiting conditions. J. Biol. Chem 278, 40612–20 10.1074/jbc.m307847200 [PubMed: 12902335]
115. Froschauer EM, Schweyen RJ, Wiesenberger G (2009) The yeast mitochondrial carrier proteins Mrs3p/Mrs4p mediate iron transport across the inner mitochondrial membrane. Biochim. Biophys. Acta Biomembr 1788, 1044–50 10.1016/j.bbamem.2009.03.004
116. Yin M, Liu Y, Chen Y (2021) Iron metabolism: an emerging therapeutic target underlying the anti-cancer effect of quercetin. Free Radic. Res 55, 296–303 10.1080/10715762.2021.1898604 [PubMed: 33818251]
117. Gao J, Zhou Q, Wu D, Chen L (2021) Mitochondrial iron metabolism and its role in diseases. Clin. Chim. Acta 513, 6–12 10.1016/j.cca.2020.12.005 [PubMed: 33309797]
118. Tsushima RG, Wickenden AD, Bouchard RA, Oudit GY, Liu PP, Backx PH (1999) Modulation of Iron Uptake in Heart by L-Type Ca^{2+} Channel Modifiers. Circ. Res 84, 1302–9. 10.1161/01.res.84.11.1302 [PubMed: 10364568]
119. Garrick MD (2011) Human iron transporters. Genes Nutr. 6, 45–54 10.1007/s12263-010-0184-8 [PubMed: 21437029]
120. Pantopoulos K, Porwal SK, Tartakoff A, Devireddy L (2012) Mechanisms of mammalian iron homeostasis. Biochemistry. 51, 5705–24 10.1021/bi300752r [PubMed: 22703180]
121. Banerjee S, Datta R (2020) Leishmania infection triggers hepcidin-mediated proteasomal degradation of Nramp1 to increase phagolysosomal iron availability. Cell. Microbiol 22, e13253 10.1111/cmi.13253 [PubMed: 32827218]
122. Tong Y, Guo M (2009) Bacterial heme-transport proteins and their heme-coordination modes. Arch. Biochem. Biophys 481, 1–15 10.1016/j.abb.2008.10.013 [PubMed: 18977196]
123. Schalk IJ, Mislin GLA, Brillet K (2012) Structure, function and binding selectivity and stereoselectivity of siderophore–iron outer membrane transporters. Curr. Top. Membr 69, 37–66 10.1016/b978-0-12-394390-3.00002-1 [PubMed: 23046646]
124. Peuckert F, Ramos-Vega AL, Miethke M, Schwörer CJ, Albrecht AG, Oberthür M, et al. (2011) The siderophore binding protein FeuA shows limited promiscuity toward exogenous triscatecholates. Chem. Biol 18, 907–19 10.1016/j.chembiol.2011.05.006 [PubMed: 21802011]
125. Li N, Zhang C, Li B, Liu X, Huang Y, Xu S, et al. (2012) Unique Iron Coordination in Iron-chelating Molecule Vibriobactin Helps Vibrio cholerae Evade Mammalian Siderocalin-mediated Immune Response. J. Biol. Chem 287, 8912–9 10.1074/jbc.M111.316034 [PubMed: 22291019]
126. Grigg JC, Vermeiren CL, Heinrichs DE, Murphy MEP (2007) Heme Coordination by Staphylococcus aureus IsdE. J. Biol. Chem 282, 28815–22 10.1074/jbc.M704602200 [PubMed: 17666394]
127. Ho WW, Li H, Eakanunkul S, Tong Y, Wilks A, Guo M, et al. (2007) Holo- and apo-bound structures of bacterial periplasmic heme-binding proteins. J. Biol. Chem 282, 35796–802 10.1074/jbc.m706761200 [PubMed: 17925389]
128. Wilde EJ, Hughes A, Blagova EV, Moroz OV, Thomas RP, Turkenburg JP, et al. (2017) Interactions of the periplasmic binding protein CeuE with Fe(III) n-LICAM4–siderophore analogues of varied linker length. Sci. Rep 7, 45941 10.1038/srep45941 [PubMed: 28383577]
129. Aisen P, Leibman A, Zweier J (1978) Stoichiometric and site characteristics of the binding of iron to human transferrin. J. Biol. Chem 253, 1930–7 10.1016/S0021-9258(19)62337-9 [PubMed: 204636]
130. Calmettes C, Alcantara J, Yu RH, Schryvers AB, Moraes TF (2012) The structural basis of transferrin sequestration by transferrin-binding protein B. Nat. Struct. Mol. Biol 19, 358–60 10.1038/nsmb.2251 [PubMed: 22343719]

131. Delepelaire P (2019) Bacterial ABC transporters of iron containing compounds. Res. Microbiol 170, 345–57 10.1016/j.resmic.2019.10.008 [PubMed: 31678562]

132. Radka CD, DeLucas LJ, Wilson LS, Lawrenz MB, Perry RD, Aller SG (2017) Crystal structure of Yersinia pestis virulence factor YfeA reveals two polyspecific metal-binding sites. Acta Crystallogr. D Struct. Biol 73, 557–72 10.1107/s2059798317006349 [PubMed: 28695856]

133. Sun X, Baker HM, Ge R, Sun H, He Q-Y, Baker EN (2009) Crystal Structure and Metal Binding Properties of the Lipoprotein MtsA, Responsible for Iron Transport in *Streptococcus pyogenes*. Biochemistry 48, 6184–90 10.1021/bi900552c [PubMed: 19463017]

134. Desrosiers Daniel C, Bearden Scott W, Mier I, Abney J, Paulley James T, Fetherston Jacqueline D, et al. (2010) Znu Is the Predominant Zinc Importer in *Yersinia pestis* during In Vitro Growth but Is Not Essential for Virulence. Infect. Immun 78, 5163–77 10.1128/IAI.00732-10 [PubMed: 20855510]

135. Billesbølle CB, Azumaya CM, Kretsch RC, Powers AS, Gonen S, Schneider S, et al. (2020) Structure of hepcidin-bound ferroportin reveals iron homeostatic mechanisms. Nature. 586, 807–11 10.1038/s41586-020-2668-z [PubMed: 32814342]

136. Nevo Y, Nelson N (2006) The NRAMP family of metal-ion transporters. Biochim. Biophys. Acta Mol. Cell. Res 1763, 609–20 10.1016/j.bbamcr.2006.05.007

137. Yang Z, Yang F, Liu JL, Wu HT, Yang H, Shi Y, et al. (2022) Heavy metal transporters: Functional mechanisms, regulation, and application in phytoremediation. Sci. Total Environ 809, 151099 10.1016/j.scitotenv.2021.151099 [PubMed: 34688763]

138. Ullah I, Wang Y, Eide DJ, Dunwell JM (2018) Evolution, and functional analysis of Natural Resistance-Associated Macrophage Proteins (NRAMPs) from *Theobroma cacao* and their role in cadmium accumulation. Sci. Rep 8, 14412 10.1038/s41598-018-32819-y [PubMed: 30258092]

139. McCabe SM, Zhao N (2021) The Potential Roles of Blood-Brain Barrier and Blood-Cerebrospinal Fluid Barrier in Maintaining Brain Manganese Homeostasis. Nutrients 13(6), 1833 10.3390/nu13061833 [PubMed: 34072120]

140. Boyer E, Bergevin I, Malo D, Gros P, Cellier MFM (2002) Acquisition of Mn(II) in Addition to Fe(II) Is Required for Full Virulence of *Salmonella enterica Serovar Typhimurium*. Infect. Immun 70, 6032–42 10.1128/iai.70.11.6032-6042.2002 [PubMed: 12379679]

141. Janulczyk R, Ricci S, Björck L (2003) MtsABC is important for manganese and iron transport, oxidative stress resistance, and virulence of *Streptococcus pyogenes*. Infect. Immun 71, 2656–64 10.1128/IAI.71.5.2656-2664.2003 [PubMed: 12704140]

142. Paik S, Brown A, Munro CL, Cornelissen CN, Kitten T (2003) The sloABCR operon of Streptococcus mutans encodes an Mn and Fe transport system required for endocarditis virulence and its Mn-dependent repressor. J. Bacteriol 185, 5967–75 10.1128/jb.185.20.5967-5975.2003 [PubMed: 14526007]

143. Begg SL, Eijkelkamp BA, Luo Z, Couñago RM, Morey JR, Maher MJ, et al. (2015) Dysregulation of transition metal ion homeostasis is the molecular basis for cadmium toxicity in *Streptococcus pneumoniae*. Nature Commun. 6, 6418 10.1038/ncomms7418 [PubMed: 25731976]

144. Singh KV, Coque TM, Weinstock GM, Murray BE (1998) In vivo testing of an Enterococcus faecalis efaA mutant and use of efaA homologs for species identification. FEMS Immunol. Med. Microbiol 21, 323–31 10.1111/j.1574-695x.1998.tb01180.x [PubMed: 9753005]

145. Gat O, Mendelson I, Chitlaru T, Ariel N, Altboum Z, Levy H, et al. (2005) The solute-binding component of a putative Mn(II) ABC transporter (MntA) is a novel *Bacillus anthracis* virulence determinant. Mol. Microbiol 58, 533–51 10.1111/j.1365-2958.2005.04848.x [PubMed: 16194238]

146. Gribenko A, Mosyak L, Ghosh S, Parris K, Svenson K, Moran J, et al. (2013) Three-dimensional structure and biophysical characterization of *Staphylococcus aureus* cell surface antigen-manganese transporter MntC. J. Mol. Biol 425, 3429–45 10.1016/j.jmb.2013.06.033 [PubMed: 23827136]

147. Sun H, Xu G, Zhan H, Chen H, Sun Z, Tian B, et al. (2010) Identification and evaluation of the role of the manganese efflux protein in *Deinococcus radiodurans*. BMC Microbiol. 10, 319 10.1186/1471-2180-10-319 [PubMed: 21156049]

148. Zeinert R, Martinez E, Schmitz J, Senn K, Usman B, Anantharaman V, et al. (2018) Structure-function analysis of manganese exporter proteins across bacteria. J. Biol. Chem 293, 5715–30 10.1074/jbc.M117.790717 [PubMed: 29440394]

149. Allen GS, Wu CC, Cardozo T, Stokes DL (2011) The architecture of CopA from Archeaoglobus fulgidus studied by cryo-electron microscopy and computational docking. Structure 19, 1219–32 10.1016/j.str.2011.05.014 [PubMed: 21820315]

150. Cohen Y, Megyeri M, Chen OCW, Condomitti G, Riezman I, Loizides-Mangold U, et al. (2013) The yeast p5 type ATPase, spf1, regulates manganese transport into the endoplasmic reticulum. PloS one 8, e85519 10.1371/journal.pone.0085519 [PubMed: 24392018]

151. Tomita A, Daiho T, Kusakizako T, Yamashita K, Ogasawara S, Murata T, et al. (2021) Cryo-EM reveals mechanistic insights into lipid-facilitated polyamine export by human ATP13A2. Mol. Cell 81, 4799–809.e5 10.1016/j.molcel.2021.11.001 [PubMed: 34798056]

152. Garcia AWA, Kinskovski UP, Diehl C, Reuwsaat JCV, Motta de Souza H, Pinto HB, et al. (2020) Participation of Zip3, a ZIP domain-containing protein, in stress response and virulence in *Cryptococcus gattii*. Fungal Genet. Biol 144, 103438 10.1016/j.fgb.2020.103438 [PubMed: 32738289]

153. Sorribes-Dauden R, Peris D, Martínez-Pastor MT, Puig S (2020) Structure and function of the vacuolar Ccc1/VIT1 family of iron transporters and its regulation in fungi. Comput. Struct. Biotechnol. J 18, 3712–22 10.1016/j.csbj.2020.10.044 [PubMed: 33304466]

154. Anderson GJ, Vulpe CD (2009) Mammalian iron transport. Cell. Mol. Life Sci 66, 3241 10.1007/s00018-009-0051-1 [PubMed: 19484405]

155. Huang Y, Lemieux MJ, Song J, Auer M, Wang DN (2003) Structure and mechanism of the glycerol-3-phosphate transporter from *Escherichia coli*. Science 301, 616–20. 10.1126/science.1087619 [PubMed: 12893936]

156. Crossgrove JS, Allen DD, Bukaveckas BL, Rhineheimer SS, Yokel RA (2003) Manganese distribution across the blood-brain barrier. I. Evidence for carrier-mediated influx of managanese citrate as well as manganese and manganese transferrin. Neurotoxicology 24, 3–13 10.1016/s0161-813x(02)00089-x [PubMed: 12564377]

157. Erikson KM, Thompson K, Aschner J, Aschner M (2007) Manganese neurotoxicity: a focus on the neonate. Pharmacol. Ther 113, 369–77 10.1016/j.pharmthera.2006.09.002 [PubMed: 17084903]

158. Sauer DB, Song J, Wang B, Hilton JK, Karpowich NK, Mindell JA, et al. (2021) Structure and inhibition mechanism of the human citrate transporter NaCT. Nature 591, 157–61 10.1038/s41586-021-03230-x [PubMed: 33597751]

159. Wu M, Tong S, Waltersperger S, Diederichs K, Wang M, Zheng L (2013) Crystal structure of Ca^{2+}/H^{+} antiporter protein YfkE reveals the mechanisms of Ca^{2+} efflux and its pH regulation. Proc. Natl. Acad. Sci. U. S. A 110, 11367–72 10.1073/pnas.1302515110 [PubMed: 23798403]

160. Crossgrove JS, Yokel RA (2005) Manganese distribution across the blood-brain barrier. IV. Evidence for brain influx through store-operated calcium channels. Neurotoxicology 26, 297–307 10.1016/j.neuro.2004.09.004 [PubMed: 15935202]

161. Hohle TH, O'Brian MR (2014) Magnesium-dependent processes are targets of bacterial manganese toxicity. Mol. Microbiol 93, 736–47 10.1111/mmi.12687 [PubMed: 24975873]

162. Daniel H, Spanier B, Kottra G, Weitz D (2006) From Bacteria to Man: Archaic Proton-Dependent Peptide Transporters at Work. Physiology 21, 93–102 10.1152/physiol.00054.2005 [PubMed: 16565475]

163. Trilisenko L, Zvonarev A, Valiakhmetov A, Penin AA, Eliseeva IA, Ostroumov V, et al. (2019) The Reduced Level of Inorganic Polyphosphate Mobilizes Antioxidant and Manganese-Resistance Systems in *Saccharomyces cerevisiae*. Cells 8(5), 461 10.3390/cells8050461 [PubMed: 31096715]

164. Tuschl K, Mills PB, Clayton PT (2013) Manganese and the Brain. Int. Rev. Neurobiol 110, 277–312 10.1016/b978-0-12-410502-7.00013-2 [PubMed: 24209443]

165. Karki P, Lee E, Aschner M (2013) Manganese Neurotoxicity: a Focus on Glutamate Transporters. Ann. Occup. Environ. Med 25, 4 10.1186/2052-4374-25-4 [PubMed: 24472696]

166. Itoh K, Sakata M, Watanabe M, Aikawa Y, Fujii H (2008) The entry of manganese ions into the brain is accelerated by the activation of N-methyl-D-aspartate receptors. Neuroscience 154, 732–40 10.1016/j.neuroscience.2008.03.080 [PubMed: 18495352]

167. Lü W, Du J, Goehring A, Gouaux E (2017) Cryo-EM structures of the triheteromeric NMDA receptor and its allosteric modulation. Science 355 10.1126/science.aal3729

168. Erikson K, Aschner M (2002) Manganese Causes Differential Regulation of Glutamate Transporter (GLAST) Taurine Transporter and Metallothionein in Cultured Rat Astrocytes. NeuroToxicology 23, 595–602 10.1016/S0161-813X(02)00012-8 [PubMed: 12428731]

169. Lee E, Sidoryk-Wêgrzynowicz M, Wang N, Webb A, Son DS, Lee K, et al. (2012) GPR30 regulates glutamate transporter GLT-1 expression in rat primary astrocytes. J. Biol. Chem 287, 26817–28 10.1074/jbc.m112.341867 [PubMed: 22645130]

170. Bowman AB, Kwakye GF, Herrero Hernández E, Aschner M (2011) Role of manganese in neurodegenerative diseases. J. Trace Elem. Med. Biol 25, 191–203 10.1016/j.jtemb.2011.08.144 [PubMed: 21963226]

171. Goytain A, Hines RM, Quamme GA (2008) Huntingtin-interacting proteins, HIP14 and HIP14L, mediate dual functions, palmitoyl acyltransferase and Mg^{2+} transport. J. Biol. Chem 283, 33365–74 10.1074/jbc.m801469200 [PubMed: 18794299]

172. Anderson JG, Cooney PT, Erikson KM (2007) Inhibition of DAT function attenuates manganese accumulation in the globus pallidus. Environ. Toxicol. Pharmacol 23, 179–84 10.1016/j.etap.2006.08.006 [PubMed: 17387379]

173. Levenson CW, Tassabehji NM (2004) Iron and ageing: an introduction to iron regulatory mechanisms. Ageing Res. Rev 3, 251–63 10.1016/j.arr.2004.03.001 [PubMed: 15231236]

174. Puig S, AndrÉS-ColÁS N, GarcÍA-Molina A, PeÑArrubia L (2007) Copper and iron homeostasis in Arabidopsis: responses to metal deficiencies, interactions and biotechnological applications. Plant Cell Environ. 30, 271–90 10.1111/j.1365-3040.2007.01642.x [PubMed: 17263774]

175. Montalbetti N, Simonin A, Kovacs G, Hediger MA (2013) Mammalian iron transporters: families SLC11 and SLC40. Mol. Aspects Med 34, 270–87 10.1016/j.mam.2013.01.002 [PubMed: 23506870]

176. Yanatori I, Kishi F (2019) DMT1 and iron transport. Free Radic. Biol. Med 133, 55–63 10.1016/j.freeradbiomed.2018.07.020 [PubMed: 30055235]

177. Fetherston JD, Bertolino VJ, Perry RD (1999) YbtP and YbtQ: two ABC transporters required for iron uptake in *Yersinia pestis*. Mol. Microbiol 32, 289–99 10.1046/j.1365-2958.1999.01348.x [PubMed: 10231486]

178. Bearden SW, Perry RD (1999) The Yfe system of Yersinia pestis transports iron and manganese and is required for full virulence of plague. Mol. Microbiol 32, 403–14 10.1046/j.1365-2958.1999.01360.x [PubMed: 10231495]

179. Brem D, Pelludat C, Rakin A, Jacobi CA, Heesemann J (2001) Functional analysis of yersiniabactin transport genes of *Yersinia enterocolitica*. Microbiology 147, 1115–27 10.1099/00221287-147-5-1115 [PubMed: 11320115]

180. Pattery T, Hernalsteens JP, De Greve H (1999) Identification and molecular characterization of a novel Salmonella enteritidis pathogenicity islet encoding an ABC transporter. Mol. Microbiol 33, 791–805 10.1046/j.1365-2958.1999.01526.x [PubMed: 10447888]

181. Clarke TE, Braun V, Winkelmann G, Tari LW, Vogel HJ (2002) X-ray crystallographic structures of the *Escherichia coli* periplasmic protein FhuD bound to hydroxamate-type siderophores and the antibiotic albomycin. J. Biol. Chem 277, 13966–72 10.1074/jbc.m109385200 [PubMed: 11805094]

182. Tom-Yew SAL, Cui DT, Bekker EG, Murphy MEP (2005) Anion-independent Iron Coordination by the Campylobacter jejuni Ferric Binding Protein. J. Biol. Chem 280, 9283–90. 10.1074/jbc.M412479200 [PubMed: 15613474]

183. Brown JS, Gilliland SM, Holden DW (2001) A *Streptococcus pneumoniae* pathogenicity island encoding an ABC transporter involved in iron uptake and virulence. Mol. Microbiol 40, 572–85 10.1046/j.1365-2958.2001.02414.x [PubMed: 11359564]

184. Chhabra R, Saha A, Chamani A, Schneider N, Shah R, Nanjundan M (2020) Iron Pathways and Iron Chelation Approaches in Viral, Microbial, and Fungal Infections. Pharmaceuticals 13(10), 275 10.3390/ph13100275 [PubMed: 32992923]

185. Rodriguez GM, Smith I (2006) Identification of an ABC transporter required for iron acquisition and virulence in *Mycobacterium tuberculosis*. J. Bacteriol 188, 424–30 10.1128/jb.188.2.424-430.2006 [PubMed: 16385031]

186. Zhang B, Rao Z, Yang H, Sun S, Gao Y, Yang X, et al. (2022) Structural insights as to how iron-loaded siderophores are imported into *Mycobacterium tuberculosis* by IrtAB. bioRxiv 10.1101/2022.01.11.475891

187. Cheng W, Li Q, Jiang YL, Zhou CZ, Chen Y (2013) Structures of *Streptococcus pneumoniae* PiaA and its complex with ferrichrome reveal insights into the substrate binding and release of high affinity iron transporters. PLoS One. 8, e71451 10.1371/journal.pone.0071451 [PubMed: 23951167]

188. Zuo J, Wu Z, Li Y, Shen Z, Feng X, Zhang M, et al. (2017) Mitochondrial ABC Transporter ATM3 Is Essential for Cytosolic Iron-Sulfur Cluster Assembly. Plant Physiol. 173, 2096–109 10.1104/pp.16.01760 [PubMed: 28250070]

189. Lee JY, Yang JG, Zhitnitsky D, Lewinson O, Rees DC (2014) Structural basis for heavy metal detoxification by an Atm1-type ABC exporter. Science 343, 1133–6 10.1126/science.1246489 [PubMed: 24604198]

190. Balk J, Pilon M (2011) Ancient and essential: the assembly of iron–sulfur clusters in plants. Trends Plant Sci. 16, 218–26 10.1016/j.tplants.2010.12.006 [PubMed: 21257336]

191. Kushnir S, Babiychuk E, Storozhenko S, Davey MW, Papenbrock J, De Rycke R, et al. (2001) A Mutation of the Mitochondrial ABC Transporter Sta1 Leads to Dwarfism and Chlorosis in the Arabidopsis Mutant starik. Plant Cell 13, 89–100 10.1105/tpc.13.1.89 [PubMed: 11158531]

192. Mourer T, Normant V, Labbé S (2017) Heme Assimilation in *Schizosaccharomyces pombe* Requires Cell-surface-anchored Protein Shu1 and Vacuolar Transporter Abc3. J. Biol. Chem 292, 4898–912 10.1074/jbc.m117.776807 [PubMed: 28193844]

193. Pouliot B, Jbel M, Mercier A, Labbé S (2010) abc3+ encodes an iron-regulated vacuolar ABC-type transporter in *Schizosaccharomyces pombe*. Eukaryot. Cell 9, 59–73 10.1128/EC.00262-09 [PubMed: 19915076]

194. Pain D, Dancis A (2016) Roles of Fe–S proteins: from cofactor synthesis to iron homeostasis to protein synthesis. Curr. Opin. Genet. Dev 38, 45–51 10.1016/j.gde.2016.03.006 [PubMed: 27061491]

195. Yan Q, Shen Y, Yang X (2022) Cryo-EM structure of AMP-PNP-bound human mitochondrial ATP-binding cassette transporter ABCB7. J. Struct. Biol 214, 107832 10.1016/j.jsb.2022.107832 [PubMed: 35041979]

196. Jonker Johan W, Buitelaar M, Wagenaar E, van der Valk Martin A, Scheffer George L, Scheper Rik J, et al. (2002) The breast cancer resistance protein protects against a major chlorophyll-derived dietary phototoxin and protoporphyria. Proc. Natl. Acad. Sci. U.S.A 99, 15649–54 10.1073/pnas.202607599 [PubMed: 12429862]

197. Orlando BJ, Liao M (2020) ABCG2 transports anticancer drugs via a closed-to-open switch. Nat. Commun 11, 2264 10.1038/s41467-020-16155-2 [PubMed: 32385283]

198. Zhang Y, Xu Y-H, Yi H-Y, Gong J-M (2012) Vacuolar membrane transporters OsVIT1 and OsVIT2 modulate iron translocation between flag leaves and seeds in rice. Plant J. 72, 400–10 10.1111/j.1365-313X.2012.05088.x [PubMed: 22731699]

199. Erpapazoglou Z, Froissard M, Nondier I, Lesuisse E, Haguenauer-Tsapis R, Belgareh-Touzé N (2008) Substrate- and Ubiquitin-Dependent Trafficking of the Yeast Siderophore Transporter Sit1. Traffic 9, 1372–91 10.1111/j.1600-0854.2008.00766.x [PubMed: 18489705]

200. Khan AA, Quigley JG (2013) Heme and FLVCR-related transporter families SLC48 and SLC49. Mol. Aspects Med 34, 669–82 10.1016/j.mam.2012.07.013 [PubMed: 23506900]

201. Nemeth E, Ganz T (2021) Hepcidin-Ferroportin Interaction Controls Systemic Iron Homeostasis. Int. J. Mol. Sci 22(12), 6493 10.3390/ijms22126493 [PubMed: 34204327]

202. Le Blanc S, Garrick MD, Arredondo M (2012) Heme carrier protein 1 transports heme and is involved in heme-Fe metabolism. Am. J. Physiol. Cell. Physiol 302, C1780–5 10.1152/ajpcell.00080.2012 [PubMed: 22496243]

203. Parker JL, Deme JC, Kuteyi G, Wu Z, Huo J, Goldman ID, et al. (2021) Structural basis of antifolate recognition and transport by PCFT. Nature 595, 130–4 10.1038/s41586-021-03579-z [PubMed: 34040256]

204. Knutson MD (2019) Non-transferrin-bound iron transporters. Free Radic. Biol. Med 133, 101–11 10.1016/j.freeradbiomed.2018.10.413 [PubMed: 30316781]

205. Wu J, Yan Z, Li Z, Yan C, Lu S, Dong M, et al. (2015) Structure of the voltage-gated calcium channel Cav1.1 complex. Science 350, aad2395 10.1126/science.aad2395 [PubMed: 26680202]

206. Curie C, Cassin G, Couch D, Divol F, Higuchi K, Le Jean M, et al. (2009) Metal movement within the plant: contribution of nicotianamine and yellow stripe 1-like transporters. Ann. Bot 103, 1–11 10.1093/aob/mcn207 [PubMed: 18977764]

207. Kosman DJ (2003) Molecular mechanisms of iron uptake in fungi. Mol. Microbiol 47, 1185–97 10.1046/j.1365-2958.2003.03368.x [PubMed: 12603727]

208. White C, Yuan X, Schmidt PJ, Bresciani E, Samuel TK, Campagna D, et al. (2013) HRG1 is essential for heme transport from the phagolysosome of macrophages during erythrophagocytosis. Cell Metab. 17, 261–70 10.1016/j.cmet.2013.01.005 [PubMed: 23395172]

209. Kumar H, Finer-Moore JS, Jiang X, Smirnova I, Kasho V, Pardon E, et al. (2018) Crystal Structure of a ligand-bound LacY-Nanobody Complex. Proc. Natl. Acad. Sci. U. S. A 115, 8769–74 10.1073/pnas.1801774115 [PubMed: 30108145]

210. Caza M, Kronstad J (2013) Shared and distinct mechanisms of iron acquisition by bacterial and fungal pathogens of humans. Front. Cell. Infect. Microbiol 3, 80 10.3389/fcimb.2013.00080 [PubMed: 24312900]

211. Neumann W, Hadley RC, Nolan EM (2017) Transition metals at the host–pathogen interface: how Neisseria exploit human metalloproteins for acquiring iron and zinc. Essays Biochem. 61, 211–23 10.1042/EBC20160084 [PubMed: 28487398]

212. Eckenroth BE, Steere AN, Chasteen ND, Everse SJ, Mason AB (2011) How the binding of human transferrin primes the transferrin receptor potentiating iron release at endosomal pH. Proc. Natl. Acad. Sci. U. S. A 108, 13089–94 10.1073/pnas.1105786108 [PubMed: 21788477]

213. Kell DB, Heyden EL, Pretorius E (2020) The Biology of Lactoferrin, an Iron-Binding Protein That Can Help Defend Against Viruses and Bacteria. Front. Immun 11, 1221 10.3389/fimmu.2020.01221

214. Suzuki YA, Lopez V, Lönnerdal B (2005) Mammalian lactoferrin receptors: structure and function. Cell. Mol. Life Sci 62, 2560–75 10.1007/s00018-005-5371-1 [PubMed: 16261254]

215. Jiang R, Lopez V, Kelleher SL, Lönnerdal B (2011) Apo- and holo-lactoferrin are both internalized by lactoferrin receptor via clathrin-mediated endocytosis but differentially affect ERK-signaling and cell proliferation in caco-2 cells. J. Cell. Physiol 226, 3022–31 10.1002/jcp.22650 [PubMed: 21935933]

216. Pilpa RM, Robson SA, Villareal VA, Wong ML, Phillips M, Clubb RT (2009) Functionally distinct NEAT (NEAr Transporter) domains within the Staphylococcus aureus IsdH/HarA protein extract heme from methemoglobin. J. Biol. Chem 284, 1166–76 10.1074/jbc.M806007200 [PubMed: 18984582]

217. Muraki N, Aono S (2015) Structural Basis for Heme Recognition by HmuT Responsible for Heme Transport to the Heme Transporter in *Corynebacterium glutamicum*. Chem. Lett 45, 24–6 10.1246/cl.150894

218. Henderson DP, Payne SM (1994) Characterization of the *Vibrio cholerae* outer membrane heme transport protein HutA: sequence of the gene, regulation of expression, and homology to the family of TonB-dependent proteins. J. Bacteriol 176, 3269–77 10.1128/jb.176.11.3269-3277.1994 [PubMed: 8195082]

219. Mey AR, Payne SM (2001) Haem utilization in Vibrio cholerae involves multiple TonB-dependent haem receptors. Mol. Microbiol 42, 835–49 10.1046/j.1365-2958.2001.02683.x [PubMed: 11722746]

220. Cobessi D, Meksem A, Brillet K (2010) Structure of the heme/hemoglobin outer membrane receptor ShuA from Shigella dysenteriae: Heme binding by an induced fit mechanism. Proteins: Struct. Funct. Bioinform 78, 286–94 10.1002/prot.22539

221. Krieg S, Huché F, Diederichs K, Izadi-Pruneyre N, Lecroisey A, Wandersman C, et al. (2009) Heme uptake across the outer membrane as revealed by crystal structures of the receptor–hemophore complex. Proc. Natl. Acad. Sci. U. S. A 106, 1045–50 10.1073/pnas.0809406106 [PubMed: 19144921]

222. Mourer T, Jacques JF, Brault A, Bisaillon M, Labbé S (2015) Shu1 is a cell-surface protein involved in iron acquisition from heme in Schizosaccharomyces pombe. J. Biol. Chem 290, 10176–90 10.1074/jbc.m115.642058 [PubMed: 25733668]

223. Anderson GJ, Frazer DM (2017) Current understanding of iron homeostasis. Am. J. Clin. Nutr 106, 1559S–66S 10.3945/ajcn.117.155804 [PubMed: 29070551]

224. Nielsen MJ, Møller HJ, Moestrup SK (2010) Hemoglobin and heme scavenger receptors. Antioxid. Redox Signal 12, 261–73 10.1089/ars.2009.2792 [PubMed: 19659436]

225. Van Gorp H, Delputte PL, Nauwynck HJ (2010) Scavenger receptor CD163, a Jack-of-all-trades and potential target for cell-directed therapy. Mol. Immunol 47, 1650–60 10.1016/j.molimm.2010.02.008 [PubMed: 20299103]

226. Ma H, Li R, Jiang L, Qiao S, Chen XX, Wang A, et al. (2021) Structural comparison of CD163 SRCR5 from different species sheds some light on its involvement in porcine reproductive and respiratory syndrome virus-2 infection in vitro. Vet. Res 52, 97 10.1186/s13567-021-00969-z [PubMed: 34193250]

227. Devireddy LR, Hart DO, Goetz DH, Green MR (2010) A Mammalian Siderophore Synthesized by an Enzyme with a Bacterial Homolog Involved in Enterobactin Production. Cell 141, 1006–17 10.1016/j.cell.2010.04.040 [PubMed: 20550936]

228. Khan A, Singh P, Srivastava A (2018) Synthesis, nature and utility of universal iron chelator – Siderophore: A review. Microbiol. Res 212-213, 103–11 10.1016/j.micres.2017.10.012 [PubMed: 29103733]

229. Roskova Z, Skarohlid R, McGachy L (2022) Siderophores: an alternative bioremediation strategy? Sci. Total Environ 819, 153144 10.1016/j.scitotenv.2022.153144 [PubMed: 35038542]

230. Moynié L, Milenkovic S, Mislin GLA, Gasser V, Malloci G, Baco E, et al. (2019) The complex of ferric-enterobactin with its transporter from *Pseudomonas aeruginosa* suggests a two-site model. Nat. Commun 10, 3673 10.1038/s41467-019-11508-y [PubMed: 31413254]

231. Yang J, Goetz D, Li JY, Wang W, Mori K, Setlik D, et al. (2002) An iron delivery pathway mediated by a lipocalin. Mol. Cell 10, 1045–56 10.1016/s1097-2765(02)00710-4 [PubMed: 12453413]

232. Yang J, Mori K, Li JY, Barasch J (2003) Iron, lipocalin, and kidney epithelia. Am. J. Physiol. Renal Physiol 285, F9–18 10.1152/ajprenal.00008.2003 [PubMed: 12788784]

233. Yu B, Cheng C, Wu Y, Guo L, Kong D, Zhang Z, et al. (2020) Interactions of ferritin with scavenger receptor class A members. J. Biol. Chem 295, 15727–41 10.1074/jbc.ra120.014690 [PubMed: 32907880]

234. Santiago C, Ballesteros A, Tami C, Martínez-Muñoz L, Kaplan GG, Casasnovas JM (2007) Structures of T Cell immunoglobulin mucin receptors 1 and 2 reveal mechanisms for regulation of immune responses by the TIM receptor family. Immunity 26, 299–310 10.1016/j.immuni.2007.01.014 [PubMed: 17363299]

235. Rolfs A, Hediger MA (1999) Metal ion transporters in mammals: structure, function and pathological implications. J. Physiol 518, 1–12 10.1111/j.1469-7793.1999.0001r.x [PubMed: 10373684]

236. Yu J, Wessling-Resnick M (1998) Structural and Functional Analysis of SFT, a Stimulator of Fe Transport. J. Biol. Chem 273, 21380–5. 10.1074/jbc.273.33.21380 [PubMed: 9694900]

237. Andrews SC, Robinson AK, Rodríguez-Quiñones F (2003) Bacterial iron homeostasis. FEMS Microbiol. Rev 27, 215–37 10.1016/s0168-6445(03)00055-x [PubMed: 12829269]

238. Stevenson B, Wyckoff EE, Payne SM (2016) *Vibrio cholerae* FeoA, FeoB, and FeoC interact to form a complex. J. Bacteriol 198, 1160–70 10.1128/JB.00930-15 [PubMed: 26833408]

239. Ash MR, Maher MJ, Guss JM, Jormakka M (2011) The initiation of GTP hydrolysis by the G-domain of FeoB: insights from a transition-state complex structure. PLoS One. 6, e23355 10.1371/journal.pone.0023355 [PubMed: 21858085]

240. Schalk IJ, Yue WW, Buchanan SK (2004) Recognition of iron-free siderophores by TonB-dependent iron transporters. Mol. Microbiol 54, 14–22 10.1111/j.1365-2958.2004.04241.x [PubMed: 15458401]

241. Shaw GC, Cope JJ, Li L, Corson K, Hersey C, Ackermann GE, et al. (2006) Mitoferrin is essential for erythroid iron assimilation. Nature 440, 96–100 10.1038/nature04512 [PubMed: 16511496]

242. Ruprecht JJ, Kunji ERS (2020) The SLC25 Mitochondrial Carrier Family: Structure and Mechanism. Trends Biochem. Sc 45, 244–58 10.1016/j.tibs.2019.11.001 [PubMed: 31787485]

243. Pebay-Peyroula E, Dahout-Gonzalez C, Kahn R, Trézéguet V, Lauquin GJ, Brandolin G (2003) Structure of mitochondrial ADP/ATP carrier in complex with carboxyatractyloside. Nature 426, 39–44 10.1038/nature02056 [PubMed: 14603310]

244. Schmiege P, Fine M, Blobel G, Li X (2017) Human TRPML1 channel structures in open and closed conformations. Nature. 550, 366–70 10.1038/nature24036 [PubMed: 29019983]

245. Dong X-P, Cheng X, Mills E, Delling M, Wang F, Kurz T, et al. (2008) The type IV mucolipidosis-associated protein TRPML1 is an endolysosomal iron release channel. Nature 455, 992–6 10.1038/nature07311 [PubMed: 18794901]

246. Carrano CJ, Raymond KN (1979) Ferric ion sequestering agents. 2. Kinetics and mechanism of iron removal from transferrin by enterobactin and synthetic tricatechols. J. Am. Chem. Soc 101, 5401–4 10.1021/ja00512a047

247. Bozzi AT, Bane LB, Zimanyi CM, Gaudet R (2019) Unique structural features in an Nramp metal transporter impart substrate-specific proton cotransport and a kinetic bias to favor import. J. Gen. Physiol 151, 1413–29 10.1085/jgp.201912428 [PubMed: 31619456]

248. Jumper J, Evans R, Pritzel A, Green T, Figurnov M, Ronneberger O, et al. (2021) Highly accurate protein structure prediction with AlphaFold. Nature 596, 583–9 10.1038/s41586-021-03819-2 [PubMed: 34265844]

249. Varadi M, Anyango S, Deshpande M, Nair S, Natassia C, Yordanova G, et al. (2022) AlphaFold Protein Structure Database: massively expanding the structural coverage of protein-sequence space with high-accuracy models. Nucleic Acids Res. 50, D439–D44 10.1093/nar/gkab1061 [PubMed: 34791371]

250. Taylor KM, Morgan HE, Smart K, Zahari NM, Pumford S, Ellis IO, et al. (2007) The emerging role of the LIV-1 subfamily of zinc transporters in breast cancer. Mol. Med 13, 396–406 10.2119/2007-00040.taylor [PubMed: 17673939]

Perspectives

- The transition metals iron and manganese are essential to life, but toxic in high abundance. Metal ion homeostasis relies on a whole array of receptor, storage, regulatory, and transport proteins. Membrane transporters transiently interact with the metal ions to shuttle them into and out of cells and between cellular compartments, enabling both organismal and cellular metal homeostasis.
- Metal binding affinity and selectivity relies on the combination of how close the coordination geometry and ligands can approach ideal parameters, and how much conformational strain is induced in the protein to produce the resulting coordination geometry.
- There are still few examples of high-resolution structures of metal transporters in complex with metals. Additional structures are needed, as are studies of the metal binding thermodynamics and the protein conformational energy landscape, to fully understand and control the homeostatic machinery of manganese and iron.

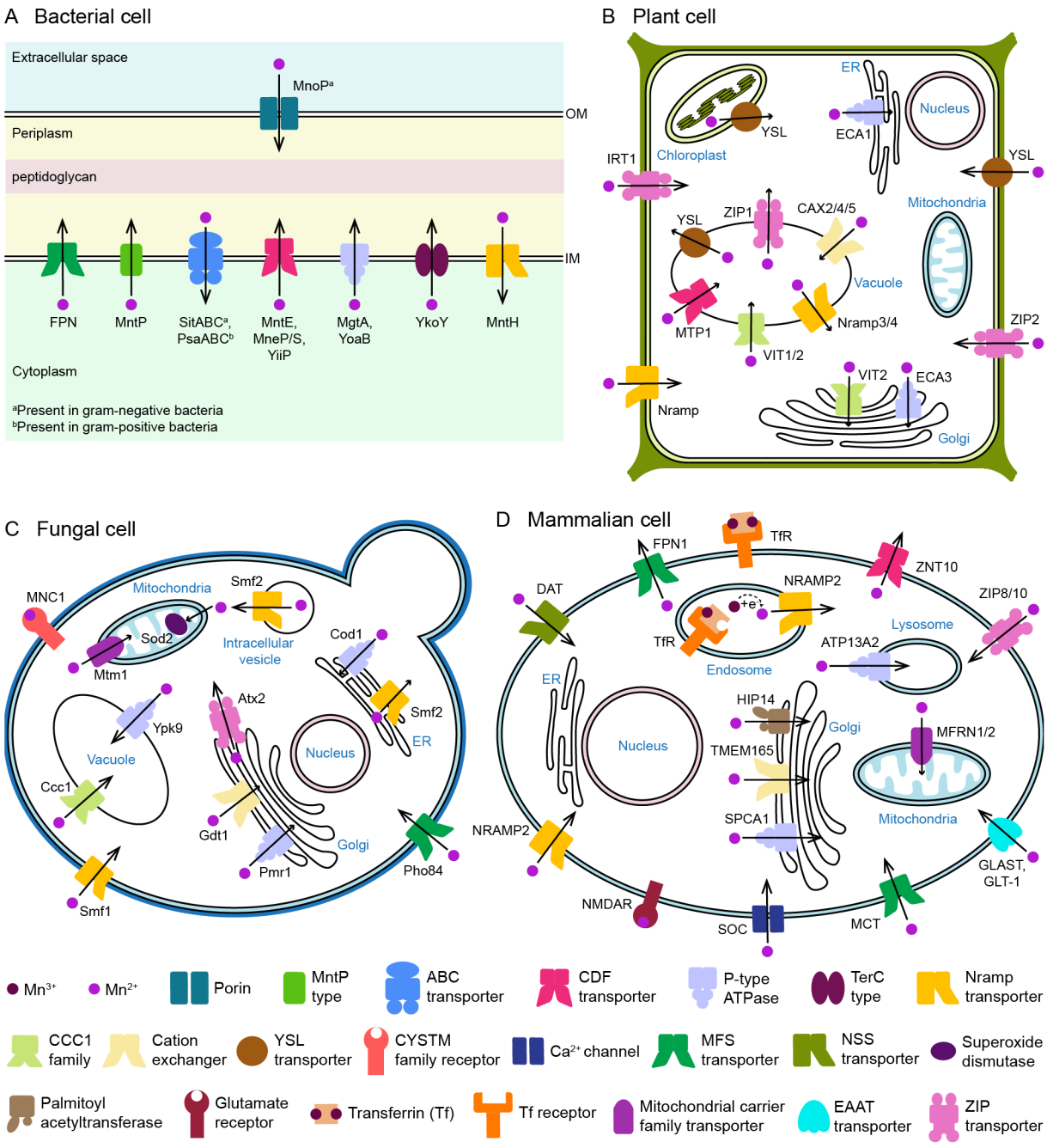

Figure 1. Transporters and receptors involved in manganese transport and homeostasis from bacteria to mammals.

(A) A gram-negative bacterial cell surface is shown as a representative for gram-positive and gram-negative bacteria because most Mn^{2+} transporters are similar in both. Mn^{2+} is imported across the OM of gram-negative bacteria mainly through porin channels like MnoP [35,161]. The illustrated ABC transporters are a representative, but not exhaustive, list (see Table 1). (B) A diagram of a plant cell highlighting transporters on the cell surface and membranes of internal organelles that regulate intracellular Mn^{2+} levels. YSL (Yellow Stripe-Like) proteins transport Mn^{2+}-chelates, all other transporters transport Mn^{2+} ions

[9,11,44]. (C) A diagram of a fungal cell highlighting transporters in the plasma membrane and organellar membranes which impact Mn^{2+} homeostasis. Mn^{2+} ions internalized into mitochondria primarily bind MnSOD (manganese-dependent superoxide dismutase), which protects against oxidative stress [2,4,52,53]. Most transporters shown have been more extensively studied in yeasts [2,51,52]. (D) In a typical mammalian cell, many plasma-membrane transporters control the cellular Mn^{2+} levels. The transferrin receptors (TfR) capture Mn^{3+}-bound transferrin and internalize it into endosomes where Mn^{3+} is converted to Mn^{2+} and transported into the cytosol by NRAMP2 [66,70,71,164]. Several transporters —some of which are not solely or even primarily dedicated to Mn^{2+} transport—have been implicated in Mn^{2+} homeostasis in the brain, including NRAMP2, ZIP8/14, ZNT10, SOC, TfR, NMDAR, glutamate transporters GLAST and GLT-1, HIP14/14L, ATP13A2, DAT, MCT [70,160,164]. In each panel, specific proteins of each transporter family are shown, and their corresponding family is indicated in the legend at the bottom (see Table 1).

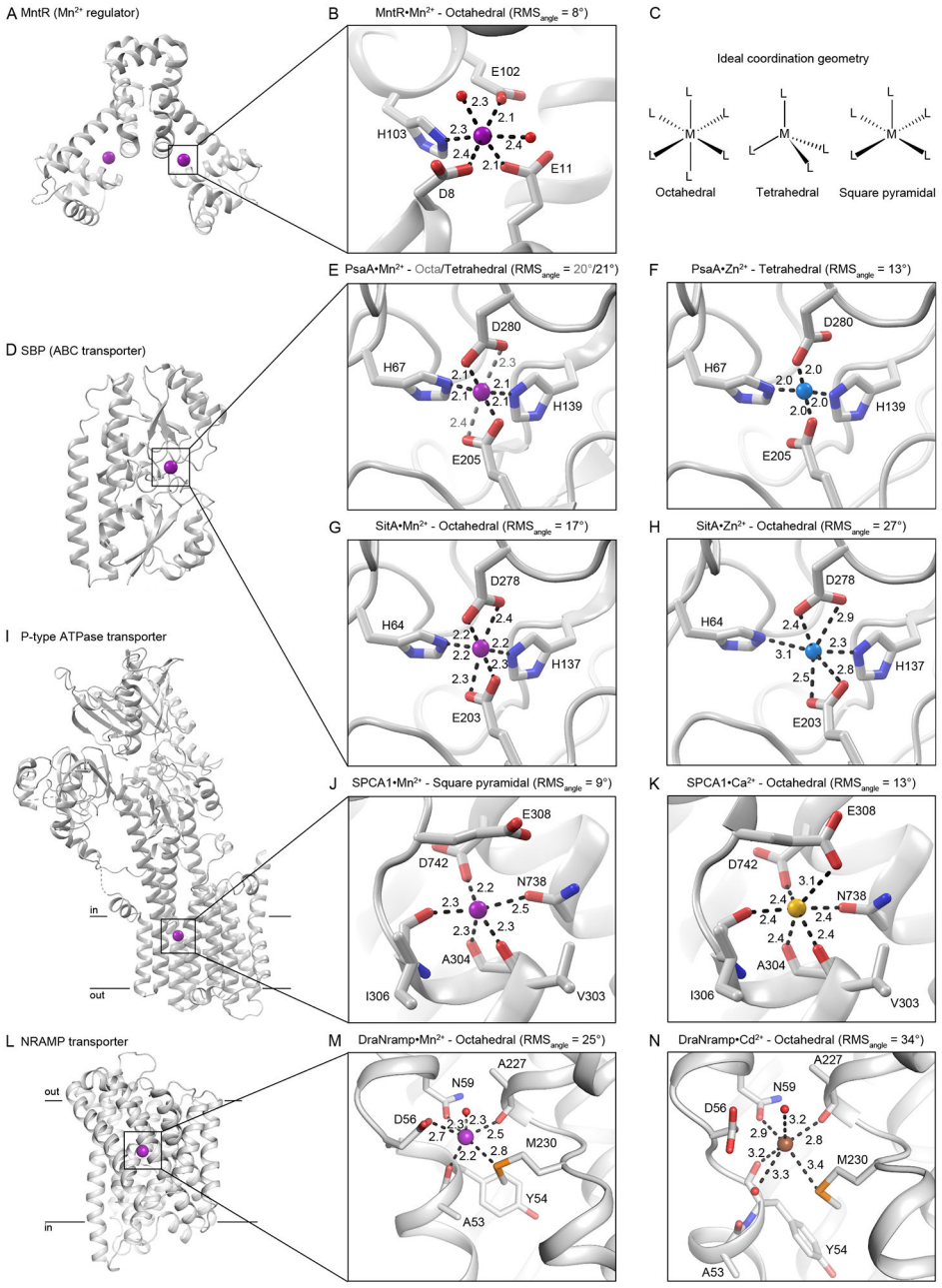

Figure 2. Coordination chemistry impacts metal uptake in Mn^{2+} transporters.

(A) Structure of a Mn^{2+} transport regulator, MntR, from *Bacillus subtilis*, bound to Mn^{2+} (PDB ID: 1ON1; [84]). (B) The six Mn^{2+} ligands form a near-ideal octahedral coordination sphere. (C) Schematic of ideal geometry for octahedral, tetrahedral, and square pyramidal coordination spheres. (D) Structure of an SBP bound to Mn^{2+} (PDB ID: 3ZTT; [74,87]). (E-F) Metal-binding site of PsaA bound to Mn^{2+} (E; PDB ID: 3ZTT) and Zn^{2+} (F; PDB ID: 1PSZ). Each coordination sphere has a distinct geometry consistent with the ion's preference: octahedral for Mn^{2+} (although two metal-oxygen bonds are longer, grey) and tetrahedral for Zn^{2+} (with the same two oxygens now more distant). The geometry is less distorted for Zn^{2+} than Mn^{2+} (for either interpretation of the structure as a the

tetrahedral-like or octahedral-like sphere), consistent with the Zn^{2+} complex being more stable (Table 2). These differences allow Mn^{2+}, the primary substrate, to be released by PsaA and transported, whereas the Zn^{2+} complex locks PsaA in a transport-incompetent closed conformation [31]. (G-H) Metal-binding site of SitA bound to Mn^{2+} (G; PDB ID: 4ORX) and Zn^{2+}(H; PDB ID: 4OXQ) [75]. Both metals are coordinated octahedrally, less distorted for Mn^{2+} compared to Zn^{2+} (Table 2), making Mn^{2+} a preferred substrate [75]. (I) Structure of a P-type ATPase, human SPCA1 (PDB ID: 7YAJ), involved in Ca^{2+} and Mn^{2+} uptake into Golgi, bound to Mn^{2+} [91]. (J-K) Metal-binding site of SPCA1 bound to Mn^{2+} (J; PDB ID: 7YAJ) and Ca^{2+} (K; PDB ID: 7YAH) [91]. Mn^{2+} binds in a square pyramidal and Ca^{2+} in an octahedral geometry. Although Mn^{2+} binds in a less favored coordination, the Mn^{2+} coordination sphere has shorter bond lengths and less angular deviation compared to the Ca^{2+} coordination, probably resulting in tighter binding than Ca^{2+} (Table 2). (L) Structure of bacterial Nramp (PDB ID: 8E60), a divalent transition metal importer [34,136], bound to its physiological substrate, Mn^{2+} [81]. (M-N) Metal-binding site of DraNramp bound to Mn^{2+} (M; PDB ID: 8E60) and Cd^{2+}(N; PDB ID: 8E6M) [81]. The coordination sphere of both metals comprises six ligands. D56—a key residue in metal and proton transport conserved across the Nramp family [76,247]—binds Mn^{2+} and not Cd^{2+}. The coordination is more distorted from ideal octahedral geometry and the bond distances are longer in the Cd^{2+} complex than in the Mn^{2+} complex (Table 2). These differences indicate that Nramps, with a broad substrate profile, display plasticity in substrate binding to transport metal ion substrates with different properties. The angular deviations from ideal geometry, calculated as root mean squared deviations (RMS_{angle}), are indicated above each illustrated binding site.

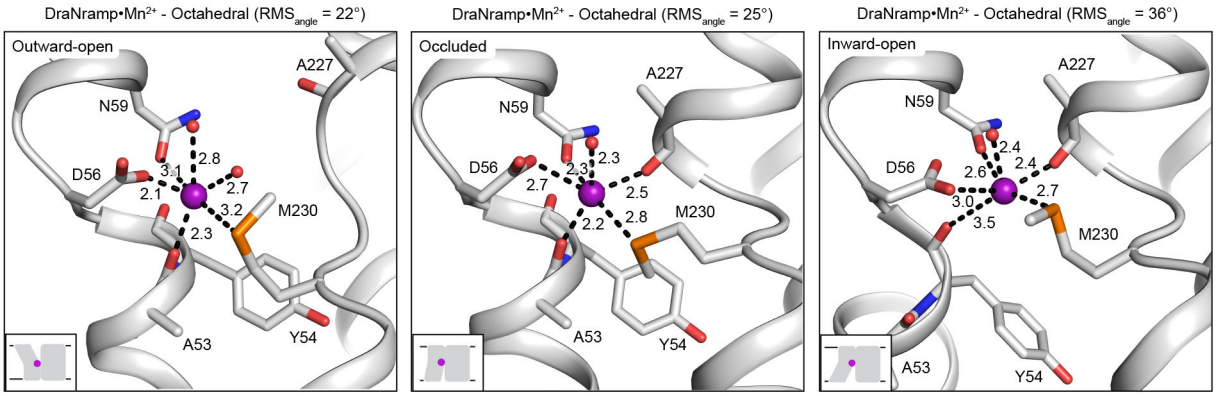

Figure 3. Coordination sphere changes across different conformations of an Nramp family Mn^{2+} transporter.

Structures of a bacterial Nramp (DraNramp) in three metal-bound conformations of the Mn^{2+} transport cycle—outward-open (PDB ID: 8E6N), occluded (PDB ID: 8E60) and inward-open (PDB ID: 8E6L)—shows that Mn^{2+} binds at the same site but with a unique coordination geometry in each of the three states [81]. Except for D56, N59 and M230, the bonding ligands vary across conformations along with the bond distances and the angular deviation (reported as RMS_{angle}). The coordination is most distorted in the inward-open conformation, which can facilitate Mn^{2+} release. These differences indicate that metal coordination can change not only for different substrates, but for different conformations of the protein bound to the same substrate.

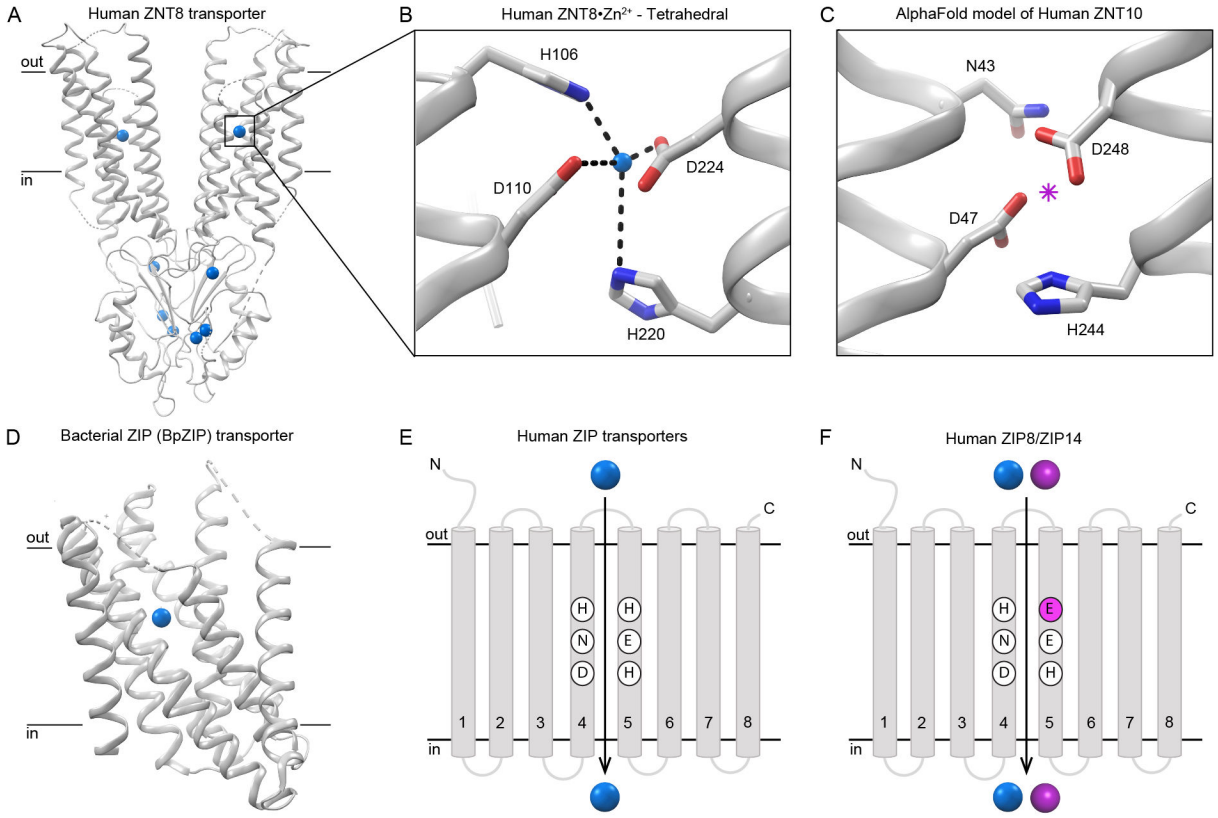

Figure 4. Mn^{2+} binding by ZNT and ZIP transporters.

(A) Structure of human ZNT8 (PDB ID: 6XPE), bound to Zn^{2+} in different domains [92]. (B) Zn^{2+}-binding site of the ZNT8 transmembrane domain with Zn^{2+} coordinated to two aspartates and two histidines in a tetrahedral geometry, a HD-HD motif conserved in most mammalian ZNTs [92]. (C) AlphaFold model of human ZNT10, a Mn^{2+} transporter, showing the residues analogous to the ZNT8 Zn^{2+}-binding site with an asparagine (N43) replacing one of the histidines, now forming a ND-HD motif [67,248,249]. Asparagine likely provides a favorable oxygen ligand and a possibility for Mn^{2+} to expand its coordination geometry from tetrahedral to preferred octahedral in ZNT10 [67,92]. (D) Structure of BpZIP, a bacterial ZIP transporter (PDB ID: 5TSA), showing a bound Zn^{2+} at the transport site [93]. (E) Topology diagram of human LIV-1 subfamily ZIP transporters, showing that Zn^{2+} is transported between TM4 and TM5, which contains the conserved metalloprotease motif (*HE*XP*H*EXGD) [67]. (F) On TM5 of ZIP8 and ZIP14, the first histidine is replaced by an asparagine, which likely enables these transporters to transport Mn^{2+} in addition to Zn^{2+} [67,93,250]. In all panels, Zn^{2+} is shown as a blue and Mn^{2+} as a magenta sphere.

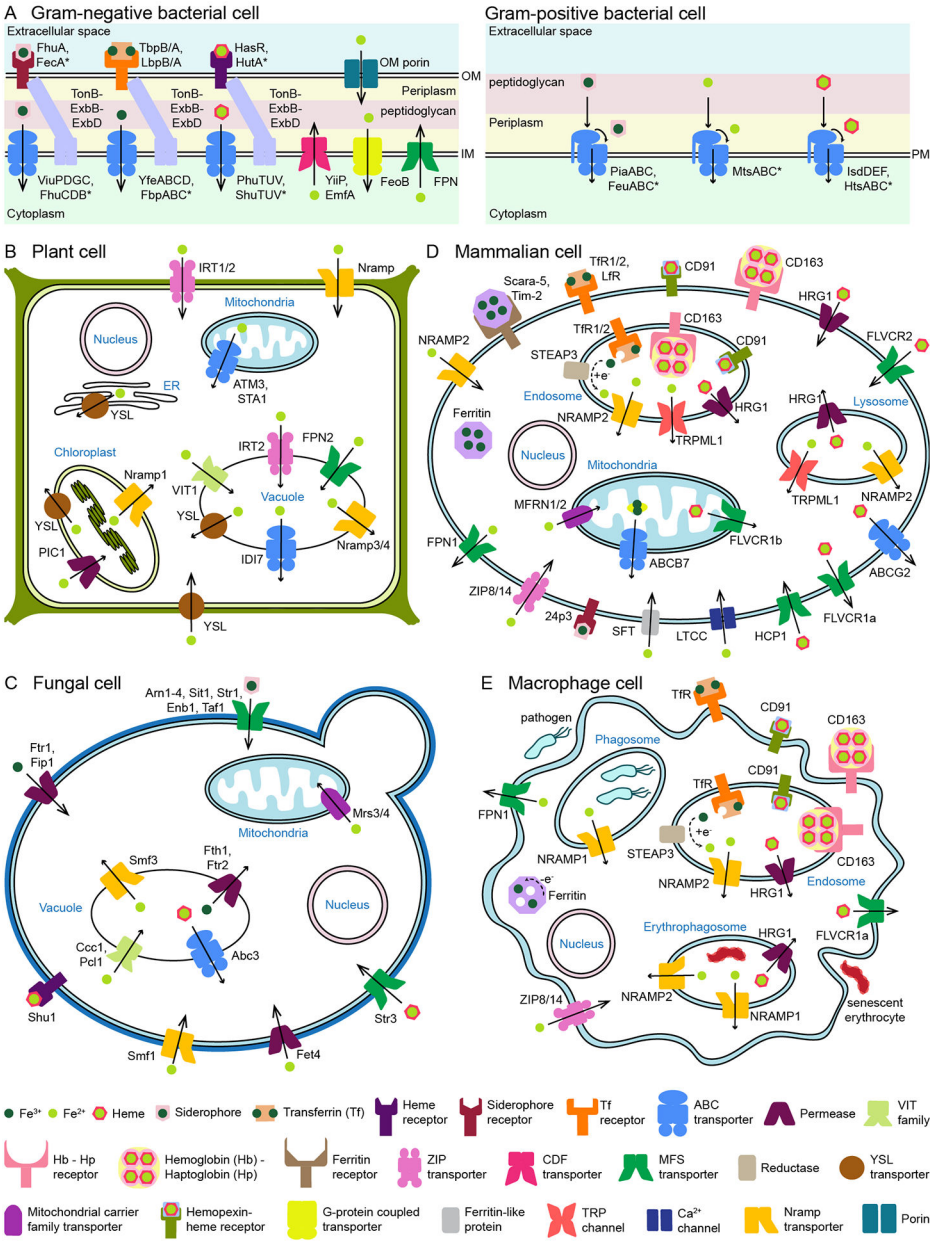

Figure 5. Transporters and receptors involved in iron transport and homeostasis from bacteria to mammals.

(A) A gram-negative bacterial cell surface (left) highlighting outer membrane (OM) and inner membrane (IM) proteins involved in transporting Fe^{2+} and Fe^{3+} either as ions or as complexes (siderophore, transferrin, heme). The periplasmic-spanning complex TonB-ExbB-ExbD energizes transport of iron from the OM to the IM [27,94,96,240]. Most of the iron transport across the IM occurs through ABC transporters [27,29,94,95]. A G-protein coupled transporter, FeoB, enables Fe^{2+} import across IM [98,99,237,238]. Ferroportin (Fpn), an MFS family transporter, exports Fe^{2+} across the IM [41]. CDF transporters, YiiP and EmfA, are also implicated in Fe^{2+} export [102,103]. In gram-positive bacteria (right), iron import is mediated by PM ABC transporters with SBPs that directly capture iron ions or complexes

[15,27,33,94]. The illustrated ABC transporters are a representative, but not exhaustive, list (see Table 3). (B) In a plant cell, iron ions are mainly transported across the cell membrane and organellar membranes by the transporters shown here [25,105,174,190]. (C) A representative fungal (yeast) cell highlighting proteins involved in ionic (Fe^{2+}/Fe^{3+}) and complexed (siderophore, heme) iron transport [2,94,110]. (D) In a typical mammalian cell, iron homeostasis is maintained by a combination of receptors—that bring iron in through endocytosis of heme, hemoglobin, transferrin, ferritin—and PM and organellar transporters [17,21,34,120]. (E) In a macrophage, iron is imported from phagosomes to the cytosol to deplete them of micronutrients as a strategy to kill engulfed pathogens, primarily by NRAMP1. A range of transporters and receptors also maintain the intracellular iron levels in macrophages [16,34,119,175]. In panels (C-E), some, but not all, oxidases and reductases that help in Fe^{2+}-Fe^{3+} interconversion during transport are shown (see text). In each panel, specific proteins of each transporter family are shown, and their corresponding family is indicated in the legend at the bottom (see Table 3).

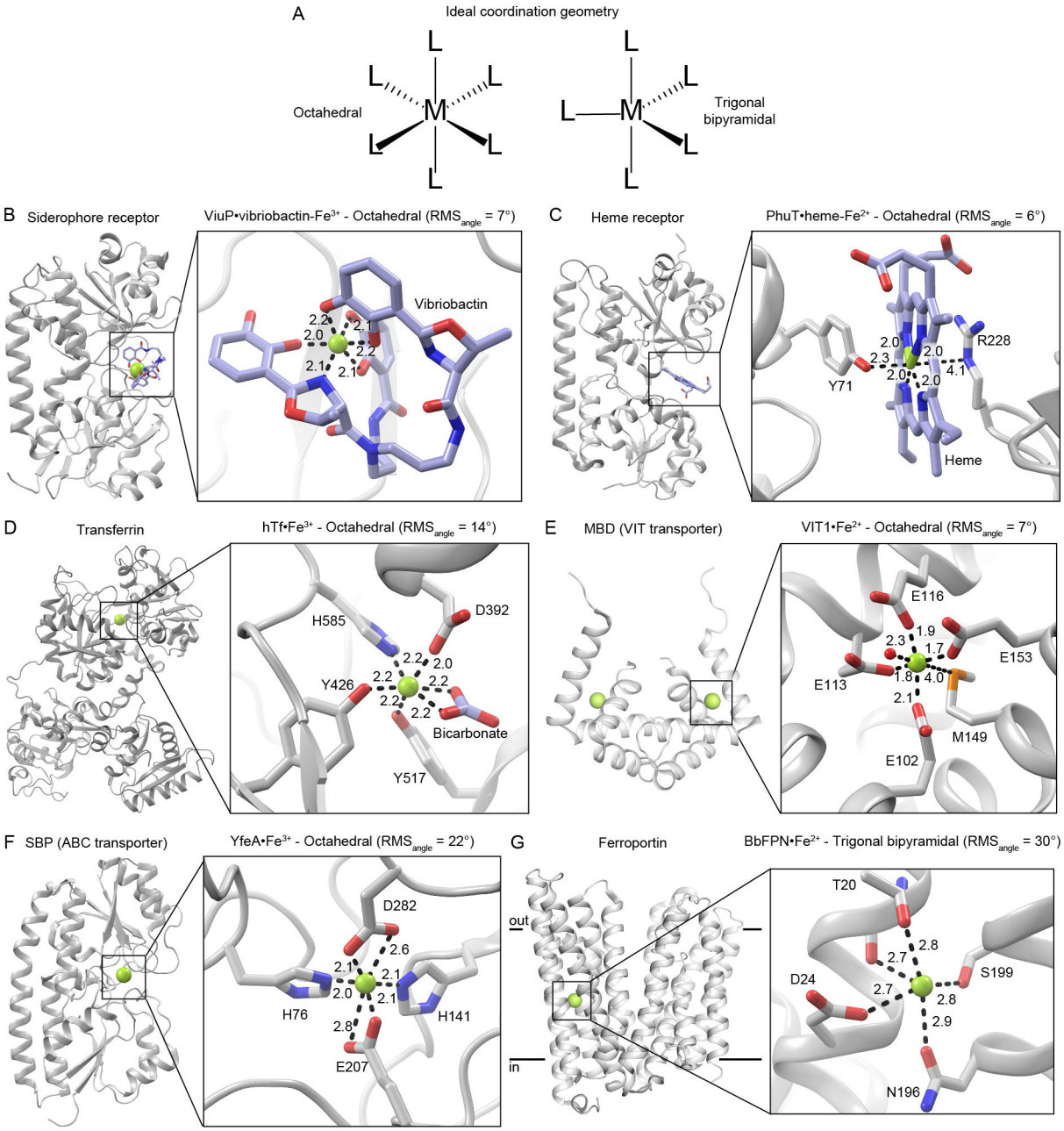

Figure 6. Iron coordination in different receptors and transporters correlates to their biological function.

(A) Schematic representation of ideal geometry for octahedral and triagonal bipyramidal coordination spheres. (B-F) Structures showing Fe^{2+} or Fe^{3+} ions coordinated by six ligands in an octahedral geometry. The structures are: the *Vibrio cholerae* siderophore receptor ViuP with its vibriobactin siderophore bound to Fe^{3+} (B; PDB ID: 3R5T; [125]), the *Pseudomonas aeruginosa* heme receptor PhuT with a bound Fe^{2+}-heme and residues Y71 and R228 completing the octahedral coordination (C; PDB ID: 2R79; [127]), human transferrin bound to Fe^{3+} (D; PDB ID: 3VE1; [130]), the metal-binding domain (MBD) of the *Eucalyptus grandis* vacuolar iron transporter 1 (VIT1) bound to Fe^{2+} (E; PDB ID: 6IU9; [50]), the SBP

of a *Yersinia pestis* ABC transporter, Yfe1, bound to Fe^{3+} (F; PDB ID: 5UYE; [132]). (G) *Bdellovibrio bacteriovorus* ferroportin (BbFPN) bound to Fe^{2+} (PDB ID: 5AYM; [41]). Five ligands coordinate Fe^{2+} in a distorted triagonal bipyramid (Table 4; [41]). BbFPN is most distorted of all the iron coordination complexes (Table 4). The extent of distortion generally correlates with the biological function in that the chelators and binders need to bind iron with high affinity so that the metal is not released until the chelators reach their destination, whereas a lower affinity enables the transporters to transport metal readily. The angular deviations from ideal geometry, calculated as root mean squared deviations (RMS_{angle}), are indicated above each illustrated binding site.

Table 1.

Transporters involved in manganese homeostasis

Family	Organism	Transporter	Function	Representative structure[a]
Nramp	Bacteria	MntH [12,13,34,136]	Mn^{2+} import	8E60
	Plants	NRAMPX[b] [10,47,137,138]	Mn^{2+} import at PM and vacuoles of roots and leaves	8E60
	Fungi[c]	Smf1/2 [34,55,136]	Mn^{2+} import across PM and ER membrane	8E60
	Animals	NRAMP2 [9,34,66,136,139]	Mn^{2+} import into cytosol through PM and endosomes	8E60
	Animals	NRAMP1 [34,136]	Import Mn^{2+} into cytosol at phagosomal membrane	8E60
ABC transporter[d]	Gram-negative bacteria	SitABCD [97,140], MntABC [89]	Mn^{2+} import into cytosol and full virulence	4OXR
	Gram-positive bacteria	MtsABC [141], SloABC [142], PsaABC [31,74,143], EfaCBA [144], MntABC [13,33,145,146], SitABC [75]	Mn^{2+} import into cytosol and virulence	3ZTT
CDF	Bacteria	MntE [147], MneP/S [13,148], EmfA [103], YiiP [36,37]	Mn^{2+} export	2QFI[e]
	Plants	MTP1 [9,47,109]	Mn^{2+} export from cytosol into vacuole of roots, leaves	6XPE[e]
	Animals	ZNT10 [67,92,139]	Mn^{2+} export across PM in liver, intestine, and brain	6XPE[e]
P-type ATPase	Bacteria	MgtA, YoaB [12,13]	Mn^{2+} export	7YAJ
	Plants	ECA1, ECA3 [9,47,109,149]	Mn^{2+} uptake in ER (ECA1) and Golgi (ECA3) of roots	7YAJ
	Fungi[c]	Pmr1p [2,51,52,55], Ypk9p [51,59], Cod1p [51,150]	Mn^{2+} export from cytosol into Golgi (Pmr1p), vacuole (Ypk9p) and ER (Cod1p)	7YAJ
	Animals	SPCA1/2 [8,69]	Mn^{2+} export from cytosol into Golgi	7YAJ
	Animals	ATP13A2 [3,68,71,139,151]	Mn^{2+} export into lysosome in brain	7VPI[f]
ZIP	Plants	IRT1 [47,109], ZIP1/2 [11,45]	Mn^{2+} import into cytosol from PM and vacuole (ZIP1) in roots	5TSB[g]
	Fungi[c]	Atx2 [51,57,58,152]	Mn^{2+} import into cytosol from Golgi	5TSB[g]
	Animals	ZIP8, ZIP14 [3,67,71,139]	Mn^{2+} import across PM in liver and brain	5TSB[g]
CCC1	Fungi[c]	Ccc1 [9,55,153]	Mn^{2+} export from cytosol into vacuole	6IU5[e]
	Plants, Fungi[c]	VIT1/2 [48-50,138]	Mn^{2+} export from cytosol into vacuoles and Golgi	6IU5[e]
MFS transporter	Bacteria, Animals	ferroportin [71,77,116,154]	Mn^{2+} export	5AYM[h]
	Fungi[c]	Pho84 [51,53,56,155]	Mn^{2+} import into cytosol across PM	7SP5[f]
	Animals	MCT [71,156-158]	Mn^{2+}-citrate complex import into cytosol in brain	7JSJ[f]
Cation exchanger	Plants	CAX2/4/5 [46,47,159]	Mn^{2+} export out of cytosol into vacuole	4KPP[i]

Family	Organism	Transporter	Function	Representative structure[a]
	Fungi[c]	Gdt1p [51,60,61]	Mn^{2+} export out of cytosol into Golgi	4KPP[i]
	Animals	TMEM165 (36, 66, 67)	Mn^{2+} export out of cytosol into Golgi	4KPP[i]
Ca^{2+} channel	Animals	SOC [3,66,71,160]	Mn^{2+} import across PM in the brain	3JBR[i]
Porin	Gram-negative bacteria	MnoP [35,161]	Mn^{2+} import through OM	2POR[i]
MntP type	Bacteria	MntP [12,13,43,148]	Mn^{2+} export	-
TerC type	Bacteria	YkoY [12,13,38]	Mn^{2+} export	-
Oligopeptide transporter[d]	Plants	YSL [9,11,44,53,162]	Complexed manganese import at chloroplast, vacuole, and PM	-
CYSTM	Fungi[c]	MNC1 [55,163]	Mn^{2+} chelation and import into cytosol	-
Transferrin receptor	Animals	TfR [3,66,70,71,164]	Internalization of Mn^{3+}-transferrin	3S9L[h]
Glutamate receptor	Animals	NMDAR [165-167]	Mn^{2+} import into cytosol across blood-brain barrier	5UP2[f]
EAAT	Animals	GLAST [165,168], GLT-1 [165,169]	Mn^{2+} import that causes neurotoxicity	6X12[f]
Palmitoyl acyltransferase	Animals	HIP14/14L [3,170,171]	Mn^{2+} export from cytosol into Golgi in the brain	3EU9[f]
NSS	Animals	DAT [71,172,173]	Mn^{2+} import into cytosol across PM in the brain	4XP1[f]
Mitochondrial carrier family transporter	Fungi[c]	Mtm1 [52,62]	Mn^{2+} import from cytosol into mitochondria	1OKC[e]
	Mammals	MFRN1/2 [28,72]	Mn^{2+} import from cytosol into mitochondria	1OKC[e]

[a] The most relevant representative structure, prioritizing high-resolution structures with bound Mn^{2+}, then ones with other metal ions, then ones with no bound metal.

[b] X is a number; plants generally have 5-7 numbered NRAMP homologs.

[c] Fungi transporters are best characterized in yeasts, so yeast proteins are generally listed in this table.

[d] Non-exhaustive list.

[e] Structures with bound Zn^{2+}.

[f] Structures with no bound divalent ions at sites for transition metal transport.

[g] Structure with bound Cd^{2+}.

[h] Structure with bound iron.

[i] Structure with bound Ca^{2+}.

Table 2.

Coordination geometry of metals in the binding site of manganese transporters

Family	Protein	Organism	Substrate	PDB code (Resolution in Å) [Reference]	Coordinating atoms (number)	Coordination geometry	RMS_{angle} [a] (°)	Binding affinity [b] [Reference] [c]
Regulator	MntR	*B. subtilis*	Mn^{2+}	1ON1 (1.75 Å) [84]	NO_5 (6)	Octahedral	8	0.2 to 2 μM [83]
SBP of ABC transporter	PsaA	*S. pneumoniae*	Mn^{2+}	3ZTT [d] (2.70 Å) [87]	N_2O_2 (4)	Octahedral (Tetrahedral)	20 (21)	3.3 ± 1.0 nM [87]
			Zn^{2+}	1PSZ (2.00 Å) [74]	N_2O_2 (4)	Tetrahedral	13	231 ± 1.9 nM [87]
	SitA	*S. pseudintermedius*	Mn^{2+}	4OXR (2.00 Å) [75]	N_2O_4 (6)	Octahedral	17	N.D. [e] [75]
			Zn^{2+}	4OXQ (2.62 Å) [75]	N_2O_4 (6)	Octahedral	27	N.D. [e] [75]
P-type ATPase	SPCA1	*Homo sapiens*	Mn^{2+}	7YAJ (3.16 Å) [91]	O_5 (X)	Square pyramidal	9	0.07 ± 0.01 μM [f] [90]
			Ca^{2+}	7YAH (3.12 Å) [91]	O_6 (X)	Octahedral	13	0.13 ± 0.01 μM [f] [90]
Nramp transporter	MntH	*D. radiodurans*	Mn^{2+}	8E60 (2.38 Å) [81]	SO_5 (6)	Octahedral	25	190 ± 30 μM
			Cd^{2+}	8E6M (2.4 8Å) [81]	SO_5 (6)	Octahedral	34	55 ± 15 μM

[a] The angular deviation from ideal geometry, calculated as root mean squared deviation.

[b] Affinities (K_d) were obtained using ITC unless otherwise specified.

[c] References are listed only if they differ from those in the “PDB code" column.

[d] In this review, we interpret the geometry as octahedral based on bond length cut-offs and the authors interpret it as tetrahedral.

[e] ITC shows binding to both metals but due to fitting issues, exact K_d could not be determined, although reported to in nM range.

[f] Apparent affinities (K_m) were obtained using colorimetric ATPase assay.

Table 3.

Transporters involved in homeostasis of iron

Family	Organism	Transporter	Function	Representative structure[a]
Nramp	Plants	NRAMPX[b] [10,47,137,138,174]	Fe^{2+} import into cytosol at PM, vacuole, and chloroplast	8E60[c]
	Fungi[d]	Smf1/3 [2,34,136]	Fe^{2+} import into cytosol at PM (Smf1) and vacuole (Smf3)	8E60[c]
	Mammals	NRAMP1 [34,136,154,175]	Import of Fe^{2+} from phagosomes into cytosol	8E60[c]
	Mammals	NRAMP2 [34,136,154,175,176]	Fe^{2+} import into cytosol at PM, endosomes, and lysosomes	8E60[c]
ABC transporter	Gram-negative bacteria[e]	YbtPQ [177], YfeABCD [97,132,178], Irp6/7 [33,179], SfaABC [94,140,180], ViuPDGC [125,131], FhuCDB [131,181], FbpABC [27,182]	Fe^{2+} import and virulence	1Y4T
	Gram-positive bacteria[e]	Pit1/2 [183,184], IrtAB [185,186], PiaABC [131,187], FeuABC [124,131], MtsABC [133]	Complexed Fe^{2+} import and virulence	3HH8
	Plants	IDI7 [47,107,109]	Fe^{2+} import into cytosol from vacuolar tonoplast of leaves, stem, and flower	6G7P
	Plants	ATM3 [105,188,189] STA1 [106,190,191]	Fe^{2+} import into cytosol from mitochondria and biogenesis of Fe-S cluster	7N58[f]
	Fungi[d]	Abc3 [110,192,193]	Heme import into cytosol from vacuole	3HH8
	Mammals	ABCB7 [120,154,188,194,195]	Complexed Fe^{2+} export from mitochondrial matrix	7VGF[f]
	Mammals	ABCG2 [120,196,197]	Complexed Fe^{2+} export at PM	6VXF[f]
CDF	Bacteria	YiiP [102], EmfA [103]	Fe^{2+} export	2QFI[g]
ZIP	Plants	IRT1/2 [47,105,109]	Fe^{2+} import at PM (IRT1 and IRT2) and vacuole (IRT2)	5TSB[g]
	Mammals	ZIP8, ZIP14 [15,17,119]	Import of free Fe^{2+} at PM	5TSB[g]
CCC1	Plants	VIT1 [49,50,138,198]	Fe^{2+} export from cytosol into vacuoles	6IU9
	Fungi[d]	Ccc1, Pcl1 [2,110,113]	Fe^{2+} export from cytosol into vacuoles	6IU9
MFS transporter	Fungi[d]	Arn1-4, Sit1, Enb1, Taf1, Str1/3 [2,94,110-112,199]	Internalization of Fe^{3+}-siderophore (Arn1-4, Sit1, Enb1, Taf1, Str1) / Fe^{2+}-heme (Str3)	5AYM
	Mammals	FLVCR1a/1b/2 [16,21,120,154,200]	Export out of (FLVCR1a) and import into (FLVCR1b/2) cytosol of heme bound Fe^{2+} at PM (FLVCR1a/2) and mitochondria (FLVCR1b)	5AYM
	Plants	FPN2 [105,108]	Fe^{2+} import into vacuole from cytosol	5AYM
	Mammals, bacteria	FPN [15,41,77,100,101,116,154,175,201]	Fe^{2+} export out of cytosol across PM and regulation of hepcidin	5AYM

Family	Organism	Transporter	Function	Representative structure[a]
	Mammals	HCP1 [21,22,94,202,203]	Import of Fe^{2+}-heme into cytosol at PM	5AYM
Calcium channel	Mammals	LTCC [28,118,204,205]	Import of free Fe^{2+} into cytosol across PM	3JBR[g]
Porin	Gram-negative bacteria	Fe^{2+} porin [27,95]	Import of Fe^{2+} across OM	2POR[h]
Oligopeptide transporter[e]	Plants	YSL [26,206]	Complexed-iron transport across chloroplast, vacuole, ER and PM	-
Permease	Plants	PIC1 [25,105]	Fe^{2+} export from cytosol into chloroplast	6C9W[g]
	Fungi[d]	Ftr1, Fip1 [2,94,110], Fet4 [2,94,110,207]	Fe^{3+} (Ftr1, Fip1) or Fe^{2+} (Fet4) import into cytosol across PM	6C9W[g]
	Fungi[d]	Fth1, Ftr2 [2,110]	Fe^{3+} import into cytosol from vacuole	6C9W[g]
	Mammals	HRG1 [16,17,94,208,209]	Transport of Fe^{2+}-heme into cytosol from PM, endosomes, and lysosomes	6C9W[g]
Transferrin/ Lactoferrin receptor	Gram-negative bacteria	TbpA/TbpB [94,210,211]	Import of Fe^{3+}-transferrin into periplasm across OM	3V89
	Mammals	TfR1/2 [65,119,154,212], LfR [95,213-215]	Internalization of Fe^{3+}-transferrin (TfR1/2), H-ferritin (TfR1/2) and lactoferrin (LfR)	3S9L
	Gram-negative bacteria	LbpA/LbpB [94,210,211]	Import of Fe^{3+}-lactoferrin into periplasm across OM	7JRD
Heme receptor	Bacteria[e]	IsdABCH [94,126,216], HmuTUV [131,217], PhuTUV [127,131], TBUT heme receptors [218-221]	Import of Fe^{2+}-heme into periplasm across OM	2Q8Q
	Fungi[d]	Shu1 [110,192,222]	Import of Fe^{2+}-heme into cytosol	2Q8Q
	Mammals	CD91 [17,223,224]	Import of Fe^{2+}-heme in complex with hemopexin into cytosol across PM	2Q8Q
Hemoglobin receptor	Mammals	CD163 [17,223,225,226]	Import of hemoglobin bound Fe^{2+} in complex with haptoglobin into cytosol across PM	6K0L[g]
Siderophore receptor	Bacteria[e]	Fe^{3+}-siderophore receptors [123,131,227-230]	Internalization of Fe^{3+}-siderophore across OM	4HMQ
	Mammals	24p3 [120,231,232]	Fe^{3+}- siderophore import into cytosol across PM	3K3L[g]
Ferritin receptor	Mammals	Tim-2 [120,154,233,234]	H-ferritin import into cytosol across PM	2OR7
	Mammals	Scara-5 [120,154,233,234]	L-ferritin import into cytosol across PM	7BZZ
	Mammals	SFT [154,173,235,236]	Tf-dependent and independent iron uptake into cytosol across PM in the intestine	-
G-protein coupled transporter	Gram-negative bacteria	FeoB [94,98,99,237-239]	Fe^{2+} import into cytosol across IM	3K53[g]

Family	Organism	Transporter	Function	Representative structure[a]
TonB	Gram-negative bacteria	TonB-ExbB-ExbD [94,96,240]	Energizes transport of iron-complexes from OM to IM (TonB)	2GSK
			Energizes transport of iron-complexes from OM to IM (ExbB-ExbD)	5ZFP
Mitochondrial carrier family transporter	Fungi[d]	Mrs3/4 [2,110,114,115]	Fe^{2+} export from cytosol into mitochondria	1OKC[g]
	Mammals	MFRN1/2 [16,154,241-243]	Fe^{2+} export from cytosol into mitochondria	1OKC[g]
TRP channel	Mammals	TRPML1 [119,120,244,245]	Fe^{2+} export from endosomes and lysosomes into cytosol	5WJ5[g]

[a] The most relevant representative structure, prioritizing high-resolution structures with bound iron, then ones with other metal ions, then ones with no bound metal.

[b] X is a number; plants generally have 5-7 numbered NRAMP homologs.

[c] Structures with bound Mn^{2+}.

[d] Fungi transporters are best characterized in yeasts, so yeast proteins are generally listed in this table.

[e] Non-exhaustive list.

[f] Structures with no bound divalent ions at sites for transition metal transport.

[g] Structures with bound Zn^{2+}.

[h] Structures with bound Ca^{2+}.

Table 4.

Coordination geometry of iron in the binding site of transporters and receptors

Family	Protein	Organism	Substrate	PDB code (Resolution in Å) [Reference]	Coordinating atoms (number)	Coordination geometry	RMS_{angle} [a] (°)	Binding affinity [b] [Reference] [c]
Siderophore receptor	ViuP	*V. cholerae*	Fe^{3+}-vibriobactin	3R5T (1.45 Å) [125]	NO_5 (6)	Octahedral	7	-
	FeuA	*B. subtilis*	Fe^{3+}-enterobactin	2XUZ (1.90 Å) [124]	O_6 (6)	Octahedral	7	~10^{-51} M [d] [246]
	CeuE	*C. jejuni*	Fe^{3+}-catecholamide	5AD1 (1.32 Å) [128]	NO_5 (6)	Octahedral	6	-
Heme receptor	PhuT	*P. aeruginosa*	Fe^{2+}-heme	2R79 (2.40 Å) [127]	N_5O (6)	Octahedral	6	-
Transferrin	hTf	*H. sapiens*	Fe^{3+}	3VE1 (2.96 Å) [130]	NO_5 (6)	Octahedral	14	~10^{-21} M [e] [129]
MBD of VIT transporter	VIT1	*E. grandis*	Fe^{2+}	6IU9 (3.00 Å) [50]	SO_5 (6)	Octahedral	7	1.9 ± 0.4 μM [f] [49]
SBP of ABC transporter	YfeA	*Y. pestis*	Fe^{3+}	5UYE (2.09 Å) [132]	N_2O_4 (6)	Octahedral	22	17.8 ± 4.4 nM for Mn^{2+} [134]
	MtsA	*S. pyogenes*	Fe^{2+}	3HH8 (1.87 Å) [133]	N_2O_4 (6)	Octahedral	22	4.3 μM [g]
Ferroportin transporter	BbFPN	*B. bacteriovorus*	Fe^{2+}	5AYM (3.00 Å) [41]	O_5 (5)	Triagonal Bipyramidal	30	195 μM for Co^{2+}

[a] The angular deviation from ideal geometry, calculated as root mean squared deviation.

[b] Affinities (K_d) are for iron (Fe^{2+} or Fe^{3+} as indicated in the "Substrate" column) and obtained using ITC, unless otherwise specified.

[c] References are listed only if they differ from those in the "PDB code" column.

[d] K_d obtained using visible spectroscopy.

[e] K_d obtained using equilibrium dialysis studies.

[f] K_d obtained using intrinsic protein fluorescence quenching.

[g] K_d obtained using equilibrium dialysis and ICP-MS.